

AN ABSTRACT OF THE THESIS OF

Ann P. Ketter for the degree of Master of Science in Horticulture presented on December 4, 2006.

Title: Cellular Events Conditioned by the *Np* Gene of *Pisum sativum* L. in Rresponse to Reduced UV Light, Weevil Oviposition, and Bruchins.

Abstract Approved: \_\_\_\_\_

William M. Proebsting

In *Pisum*, the *Np* gene conditions two mitotic responses - to bruchid weevil oviposition on the pod and to reduced UV light. Oviposition by the weevil results in tumorous or neoplastic growth under the egg. Biochemically active compounds, called bruchins, were isolated from two bruchid insects (Doss et al, 2000). Femtomolar concentrations of bruchin result in programmed cell death (PCD) and neoplasm formation on the pod at the application site. PCD is evident at the application site within four hours and a large (several mg) neoplasm in five to seven days. Low UV light results in growth of neoplasm, termed spontaneous neoplasm (SN), over the entire surface of the pod and, as with bruchin application, appears to begins with PCD followed by mitosis. Genotypes containing *np/np* do not develop SN and respond only weakly to bruchin.

Both responses conditioned by *Np* initiate at the stomatal complex and are first detected by increased auto-fluorescence. In both cases, this is accompanied by increased peroxide/peroxidase activity first at the stomata, then radiating outward across the epidermal surface and into the mesophyll cells. Nuclei in the epidermis stained strongly for peroxide/peroxidase within 3 h of bruchin application. Nuclei in the mesophyll stained for peroxide/peroxidase by 24 h. Rose Bengal, which generates singlet oxygen, stimulated site-specific neoplasm formation on greenhouse grown pods. Lanthanum, an

inhibitor of  $\text{Ca}^{2+}$  influx, inhibited both ROS production and bruchin action.  $\text{ZnCl}_2$  inhibited ROS production and bruchin response less effectively than  $\text{LaCl}_3$ . Epidermal cell death demonstrated hallmarks of apoptosis. TUNEL demonstrated the presence of oligonucleosomal fragmentation, which is associated with PCD. Pods treated with bruchin demonstrated progressive TUNEL staining. The first areas to test positive for endogenous nuclease activity were the subsidiary cells of the stomatal complex. Transmission electron microscopy (TEM) found nuclear blebbing, chromatin condensation, mitochondrial swelling, changes in cytosol density and increased vacuolization. This work demonstrates that the bruchin and SN responses conditioned by the *Np* gene originate from similar cellular events: increased auto-fluorescence, increased peroxide/peroxidase, and PCD.

Cellular Events Conditioned by the *Np* Gene of *Pisum sativum* L. in Response to  
Reduced UV Light, Weevil Oviposition, and Bruchins.

by

Ann P. Ketter

A THESIS

submitted to

Oregon State University

in partial fulfillment of  
the requirement for the  
degree of

Master of Science

Presented December 4, 2006  
Commencement June 2007

Master of Science thesis of Ann P. Ketter presented on December 4, 2006

APPROVED:

---

Major Professor, representing Horticulture

---

Head of the Department of Horticulture

---

Dean of the Graduate School

I understand that my thesis will become part of the permanent collection of Oregon State University libraries. My signature below authorizes release of my thesis to any reader upon request.

---

Ann P. Ketter, Author

## ACKNOWLEDGEMENT

I would like to thank my major professor Bill Proebsting, and members of my committee John Fowler and Bob Doss for their time, talents, and guidance. I would like to acknowledge those individuals that have contributed unselfishly of themselves to my research and education: Ruth Martin, Luigi Meneghelli, and Nahla Bassil. Finally, I would like to express appreciation to my husband Jim Ketter and my children, Jacob, Sarah, and Luke. Without their unwavering support and faith I could never have achieved my goal and begun new endeavors.

## TABLE OF CONTENTS

	<u>Page</u>
Introduction.....	1
Materials and Methods.....	11
Results.....	17
Discussion.....	48
Conclusion .....	57
Bibliography.....	60

## LIST OF FIGURES

<u>Figure</u>	<u>Page</u>
1. Comparison.....	1
2. Stomata comparison.....	2
3. Bruchin.....	4
4. Example of response to bruchin treatment.....	5
5. Bruchin treatment of <i>Np</i> and <i>np</i> pods.....	17
6. Browning and fluorescence.....	18
7. Development of fluorescence following bruchin treatment.....	21
8. DAB stain for H <sub>2</sub> O <sub>2</sub> in bruchin treated pods.....	24
9. Rose Bengal.....	26
10. LaCl <sub>3</sub> and ZnCl <sub>2</sub> and peroxide stain.....	28
11. TUNEL controls.....	31
12. Progression of development of nuclear degradation.....	33
13. Complete TUNEL at 1 h.....	33
14. Complete TUNEL at 3 h.....	34
15. Complete TUNEL at 24 h.....	35
16. TEM.....	36
17. Spontaneous neoplasm fluorescence.....	39
18. Spontaneous neoplasm and peroxide stain.....	40
19. Complete TUNEL -UV48 h.....	43
20. Spontaneous neoplasm and EB.....	44
21. Changes in stomatal complex staining.....	46

22. Inhibition of SN.....	47
---------------------------	----

.

## LIST OF TABLES

<u>Table</u>	<u>Page</u>
1. Compounds tested on <i>Pisum</i> .....	16

## DEDICATION

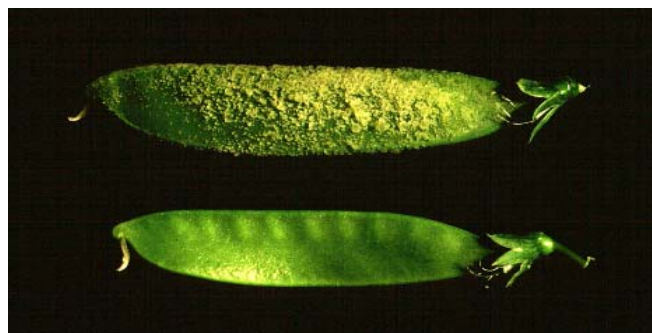
This work is dedicated to the fond memory of my undergraduate advisor Paul Jennings, of Kansas State University. His love of learning, his joy in teaching students and his respect of the natural world and science was a true inspiration. He is missed.

**Cellular events conditioned by the *Np* gene of *Pisum sativum* L. in response to reduced UV light, weevil oviposition, and bruchins.**

**Introduction**

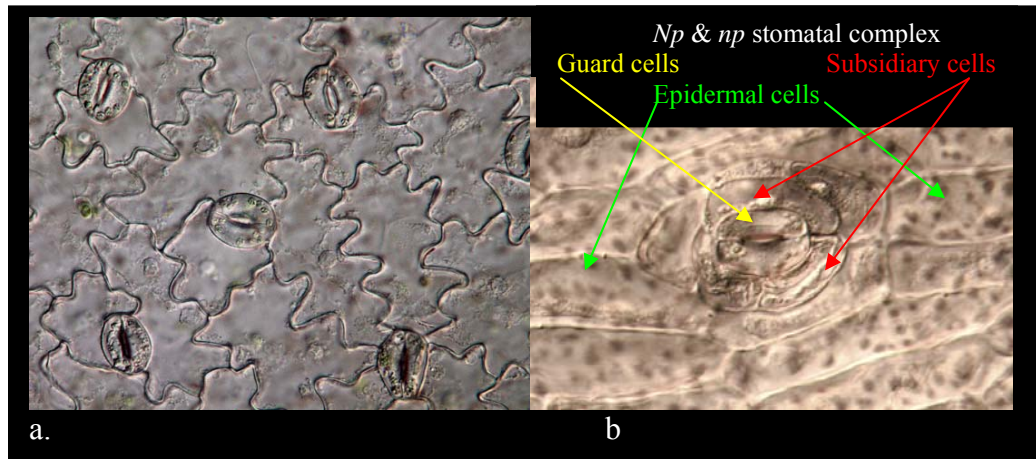
Pods of *Pisum sativum* L. homozygous or heterozygous for *Np* develop neoplastic growth across the entire surface of pods grown in a conducive environment (Fig.1), hence *Neoplastic Pod (NP)*. In a study of USDA accessions with this characteristic, the expression of neoplastic pod was induced by low light intensity, dense shade, high humidity, greenhouse culture and position of the pod on the plant (Nuttall and Lyall, 1964). It was concluded that reduction of UV light triggered neoplastic growth, a ‘pustular-like growth’ over the surface of the pod and that it was controlled by a single dominant gene, *Np*. Dodds and Matthews (1966) concluded that *Np* is common in primitive pea germplasm, including *P. humile*, *P. elatius*, and *P. fulvum*, suggesting an early evolution of the *Np* trait. This cell growth response to low UV light is referred to as spontaneous neoplasm (SN).

Fig. 1 Comparison of (top) a greenhouse grown pod and (bottom) a field grown pod.



SN originates from cells of the stomata complex found on pea pods (Snoad and Matthews, 1969). These complexes consist of: two guard cells and 4-8 subsidiary cells (Fig. 2). The subsidiary cells appear to derive from epidermal cells, not guard cells. In contrast, the stomata of the leaf, stipule, stem, pedicel, and calyx are simple, and lack subsidiary cells. Snoad and Matthews observed that the mitotic activity that resulted in neoplastic growth appeared to be limited to the subsidiary cells of the stomatal complex.

Fig. 2 Comparison of a) a stomata of the leaf and b) the stomatal complex of the pod.



An electron microscopy study of *Np* neoplasm by Burgess and Fleming (1973) characterized the subsidiary cells of the stomatal complex as smaller cells with less vacuolation than epidermal cells. The guard cells had denser cytoplasm and their plastids contained large starch accumulations. Many plasmodesmata were seen between subsidiary cells while plasmodesmata between the guard cells and subsidiary cells were not apparent. Maturing pods develop neoplasm at the stomatal subsidiary cells when grown in the greenhouse or under reduced ultraviolet light. Neoplasm was structurally similar to parenchyma cells except the plastids appeared abnormal. The earliest sign of

SN development was the apparent accumulation of “lipid material”, increased vacuolation in the subsidiary cells and development of ‘amoeboid’ nuclei. In the pre-neoplastic state, chloroplasts in the subsidiary cells were elliptical, with organized stroma and clearly defined small starch deposits. At the onset of neoplasm formation, the plastids became enlarged and more spherical in shape. All the chloroplasts in a cell changed synchronously implying genetic control. After several mitoses, the plastids degenerated and lost photosynthetic capacity, but the cells remained viable and continued to replicate.

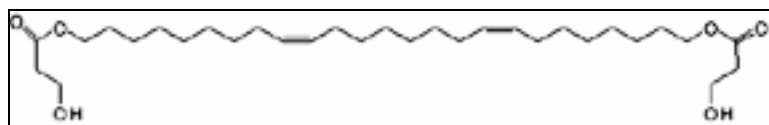
Although Dodds and Matthews (1966) could not rationalize a selective value for *Np*, this question was answered when Berdnikov, et al (1992) observed that *Np* provided resistance to pea weevil (*Bruchus pisorum* L.). They reported that callus developed under weevil eggs laid on *Np*- pods. In another study near isogenic lines of pea were used to evaluate the role of *Np* for weevil resistance. In an area heavily infested with pea weevil, 85.4% of *np/np* seed were infested and 62.2% of *Np/Np*. (Doss et al, 2000).

Berdnikov, et al (1992) also reported that weevil extracts induced callus formation at the site of application. In 1995, Doss et al reported that extracts of mature and immature female weevils, eggs and accompanying fluid as well as male weevils stimulated cell division. They found that the extract of mature females was ten times more bioactive than the extract of males and that the eggs and accompanying fluid were even more active than the mature females.

Doss et al, (2000) went on to identify a group of compounds from bruchid insects that stimulated cell division on *Np* pods. These compounds, named “bruchins”, were initially isolated from cowpea weevils (*Callosobruchus maculatus* F.). Cowpea weevils

were easier to rear than pea weevils in the quantities required to obtain sufficient bruchin for identification. Four previously unknown and biochemically active compounds were isolated from cowpea weevils and characterized (Fig. 3). The first identified was a monoester of 3-hydroxypropanoic acid and a long-chain fatty alcohol (diol). The three diesters were then identified in pea weevil extracts. The most common configuration is esterification at both oxygen atoms but there is bioactivity with only one end esterified. Two of the compounds are mono-unsaturated (C9) and two are di-unsaturated (C9&17).

Fig. 3 A bruchin molecule.

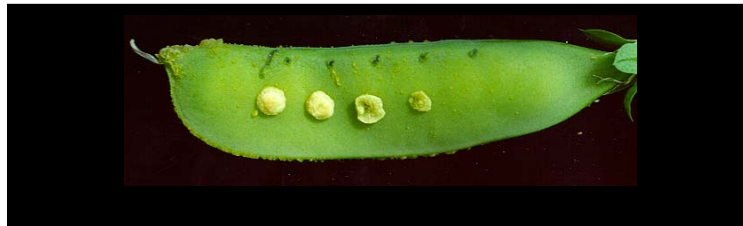


‘Bruchins are the first natural products isolated from insects that ...’ lead to cellular de-differentiation and subsequently mitosis (Doss et al, 2000). Bruchins effect a site-specific response ‘thereby mediating an effective form of induced resistance’ (Doss et al, 2000). Bruchins have been identified in two genera of bruchid adults and extracts of three additional bruchid species induced neoplasm on pea. All that is known to date about plant response to bruchin, other than *Np* peas, is that it appears to be limited to a few genotypes of *Lathyrus tingitanus* (Tangier peavine).

Bruchins proved to be potent mitogens on peas, inducing neoplasm at femtomolar concentrations. This response is dose-dependent and limited to the application site on the pod (Fig. 4). Following bruchin application, there is induction of browning in 2-6 h, swelling is evident by 24-48 h, and by 5-7 d there is enough neoplasm to remove and

weigh (several mg). Bruchins do not initiate neoplasm on stems or leaves. Homozygous recessive *np/np* responded to bruchin treatment with light browning and very moderate swelling (cell enlargement) but no neoplasm or tumor formation.

Fig. 4 An example of dose dependent *Np* response to bruchin treatment.



### Programmed Cell Death

The first visible effect of bruchin application on pea pods was browning of epidermal tissues at the application site within 2-6 h. During the work to isolate bruchins Doss et al (2000) used this browning as a cursory indicator of compound bioactivity, in part because of its rapid appearance. Following the initial browning response to bruchin application, the cells at the application site collapse within 24 hours, suggesting cell death.

Cells die by mechanisms broadly classed as either necrosis or programmed cell death (PCD). Necrosis results directly from injury such as mechanical damage or chemical toxicity that is too severe for the cells to remain viable; as such, the cells do not actively participate in their own demise (Desagher and Martinou, 2000).

In contrast, during PCD cells dismantle themselves in an organized, genetically controlled process. PCD, also called apoptosis, is essential for normal development. For

instance, PCD eliminates the extraneous cells between fingers and toes for the delineation of digits. In mice, PCD is necessary for organ definition early in embryo development. The immune system eliminates self-reactive leukocytes *en uterus* and later uses PCD to eradicate cancer cells. PCD is involved in homeostasis of tissue health by the removal of damaged and/or dead cells (Hengartner, 2000; Joza et al, 2001; Hunot and Flavell, 2001).

In mammals, there are well-established hallmarks of apoptosis: chromatin condensation, oligonucleosomal fragmentation by endogenous endonucleases, cytosol condensation, cell shrinkage, loss of cell to cell contact, blebbing of the nuclear and plasma membranes, loss of mitochondrial potential, and finally the formation of apoptotic bodies which are engulfed by phagocytes. The initial signals and mechanisms of PCD in mammals is a tightly controlled and complex process. These signals and mechanisms continue to be elucidated, but some are better understood such as the role of caspases, a family of proteases activated during PCD (Hengartner, 2000).

The mitochondria are pivotal players because they release proteins which trigger PCD, such as AIF (apoptosis inducing factor) and cytochrome c, normally confined to the intermembrane space (Lam et al, 2001; Balk and Leaver, 2001, Brenner and Kroemer, 2000). The events that confer permeability of the mitochondrial membrane are not well understood. AIF, a 57 kD flavoprotein with both a mitochondrial and nuclear signal sequence, resides in the mitochondrial intermembrane space but translocates to the nucleus upon receipt of appropriate apoptotic stimuli. There, AIF induces large-scale nuclear DNA (nDNA) fragmentation. AIF homologs are found in all three metazoan kingdoms, animal, plant, and fungus, which suggests it is an ancient orchestrator of death (Joza et al, 2001; Hunot and Favell, 2001; Desagher and Martinou, 2000).

PCD also occurs throughout plant development; germination, reproduction, and senescence, as well as being a key factor in resistance via the hypersensitive response (HR) (Pennell and Lamb, 1997; Groover et al, 1996; Greenberg 1996; Navarre and Wolpert, 1999). Recurring events in plant and animal PCD include calcium influx, vacuolar activity, and generation of reactive oxygen species (ROS). Typically, an extracellular signal triggers calcium ( $\text{Ca}^{2+}$ ) influx into the cell. Thus,  $\text{Ca}^{2+}$  channel blockers can inhibit apoptosis. There are a number of  $\text{Ca}^{2+}$  dependent reactions, endonucleases and protein kinases, which lead to the up-regulation of proteins involved in PCD (Bowler and Fluhr, 2000; Levine, 1996; Pei et al, 2000).

Vacuole collapse is an event shared by all plant PCD pathways whether for development or defense (Lam et al, 1999; Jones, 2001). Only after vacuole rupture is nuclear DNA (nDNA) nicking evident in tracheal element (TE) formation (Jones, 2001; Groover et al, 1996). Lysing agents are sequestered in the vacuole and released at the appropriate time. In plants, vacuoles absorb or digest cellular organelles and other contents prior to death and tonoplast rupture, a process called autophagy.

During HR, lesions develop at the site of pathogen entry, thereby suppressing pathogen growth (Wang et al, 1996). HR-induced defense response leads to ROS production, cell wall modifications, activation of hydrolytic enzymes, the synthesis of antimicrobial compounds (phytoalexins) and antimicrobial proteins.  $\text{H}_2\text{O}_2$  accumulation can occur in as little as two to three minutes after inoculation and cross link structural proteins of the cell wall thereby impeding pathogen progression (Thordal-Christensen 1997). Processing of the cellular corpse following HR is minimal; the toxins sequestered

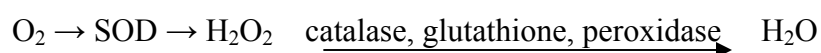
in the vacuole, phytoalexins, polyphenols, and chitinases, are released and these inhibit pathogen growth (Jones, 2001).

ROS are causative agents in PCD as signaling molecules, transcriptional triggers, and in ways still being discerned (Green and Fluhr, 1995; Allan and Fluhr, 1997; Solomon et al, 1999). Their role in PCD is highly concentration and duration dependent (Levine et al, 1994; Alvarez et al, 1998; Potikha et al, 1999; Schopfer et al, 2001).

### Reactive Oxygen Species

Reactive oxygen species (ROS), also known as reactive oxygen intermediates (ROI) and active oxygen species (AOS) play a major role in PCD. Superoxide ( $O_2^-$ ), hydrogen peroxide ( $H_2O_2$ ) and hydroxyl radical ( $OH^\cdot$ ) are most commonly encountered. Superoxides and hydroxyl radicals are extremely unstable, whereas hydrogen peroxide is more stable and membrane diffusible. In plants, disruptions of electron transport in respiration or photosynthesis generate ROS, originating from one, two, or three electron transfers to dioxygen ( $O_2$ ) (Mehdy, 1994).

ROS are produced either extracellularly by oxidases, such as peroxidases, amine oxidases, oxalate oxidase and possibly NADPH oxidase, located in the plasma membrane (PM) or cell wall (CW), or intracellularly in chloroplasts, mitochondria and peroxisomes (Schopfer et al, 2001; Mehdy, 1994). Cellular enzymatic defenses to ROS include superoxide dismutase (SOD), catalase, and glutathione peroxidase, which metabolize ROS.



Small molecule antioxidants such as ascorbate, pyruvate, flavonoids, carotenoids and glutathione also scavenge ROS and are maintained at millimolar concentrations in the cell (Green and Fluhr, 1995; Mittler et al, 1998).

ROS generation is essential for normal plant growth and development, as well as for stress and defense responses. However, oxidative damage occurs when ROS production exceeds scavenging abilities of cells (Finkel and Holbrook, 2000).

Senescence, a type of PCD, carefully shifts redox balance of the cell with the reduction of the intercellular antioxidant pool and reactive oxygen build up (Greenberg, 1996; Allen and Fluhr 1997; Bowler and Fluhr, 2000). Increasing the concentration of intracellular ROS changes the redox balance transitioning the cell metabolically and genetically to senescence/PCD. Environmental stresses such as insect or disease attack, extreme temperature, UV radiation and toxic chemicals also trigger endogenous ROS production leading to a shift in cellular redox balance (Finkel and Holbrook, 2000 Solomon et al, 1999). Elevated levels of intracellular ROS damage proteins, lipids and DNA, which can trigger PCD. Mitochondria are especially susceptible to oxidative damage, because of their proximity to ROS production. Changes in mitochondrial function and membrane permeability are fundamental to mammalian apoptosis.

Although *Np* controls cell division both in response to bruchin and to reduced UV light, there appeared to be puzzling differences. First, bruchin application results in browning (Doss et al, 2000) and cell shrinkage (Proebsting, unpublished), which suggest PCD. However, these characteristics were not observed when SN initiated. Second, Doss et al (1995) observed that neoplasm formation occurs at the site of bruchin application, whereas SN originates from stomatal complexes. As *Np* regulates both

bruchin response and SN development, I undertook a study to determine whether these phenotypes share a common cellular and physiological origin.

## Materials and Methods

### Plant Material

Lines of pea (*Pisum sativum*) homozygous for either the *Np* or *np* allele were used for all studies. These lines were selected from progeny of a single F<sub>9</sub> heterozygote from a cross between C887-332 (*Np/Np*) and I<sub>3</sub> (*np/np*). Pods used for bioassay were collected from plants grown in raised beds outdoors or grown in the greenhouse with set points of 21/16C (day/night). A minimum of three pods from three different plants were used for each assay.

### Microscopy

Epidermal peels or cross sections of pods were done dozens of times by placing tissues flat on cover slips, in water. For conventional microscopy, I used a Zeiss Axiovert microscope with differential interference contrast (DIC) optics or with epifluorescence. Digital images were acquired using a SPOT CCD camera and software (Diagnostic Instruments).

Confocal laser scanning microscopy (CLSM) used a Leica DM IRBE with 40x and 100x/NA1.4 objective, equipped with TCS 4D software and scanning package. TUNEL fluorescein and PI fluorescence was imaged using an Ar/Kr laser with the standard Leica FITC - TRITC settings. Further image processing was done in either Photoshop 5 (Adobe) or Image-Pro 4.0 (Media Cybernetics).

### Transmission electron microscopy (TEM)

Three independent rounds of TEM observations were made with pods harvested at 0, 1, 4, 12, 24 h after bruchin treatment and cut into 1-2 mm samples. Tissues were fixed in 2.5% glutaraldehyde in 0.1 M phosphate buffer, pH 7.2, vacuum infiltrated until tissues no longer floated, and left in glutaraldehyde for 2-3 hours. The fixative was removed and replaced with 0.1% phosphate buffer pH 7.2. This rinse was repeated two times to be sure all the glutaraldehyde was removed. The samples remained in the buffer overnight, then were fixed by the TEM laboratory in cacodylate, treated with OsO<sub>4</sub>, dehydrated, and embedded in resin.

### Reactive oxygen species Assays

3',3'-Diaminobenzidine (DAB) (Sigma Cat.#D8001) forms a red-brown precipitate in the presence of H<sub>2</sub>O<sub>2</sub> and peroxidase and can be viewed using light microscopy (Thordal-Christensen et al, 1997). DAB was used at 1 mg mL<sup>-1</sup> HCl to 3.8 pH (1g L<sup>-1</sup> = 0.0047 M or 4.7 mM DAB). Pods were treated with 1 μM bruchin, then at various times submerged in 4.7 mM DAB for 3 h. Ten mM ascorbic acid quenches the DAB response and was used as a negative control.

### Nitro Blue Tetrazolium

Nitro Blue Tetrazolium (NBT) (Sigma Cat.#N6976) reacts with superoxide to produce a blue precipitate. Sodium azide (NaN<sub>3</sub>)(Sigma Cat.#52002) at 10 mM, in 10 mM KH<sub>2</sub>PO<sub>4</sub>, pH 7.8, was vacuum infiltrated into pods to prevent endogenous quenching of superoxide then the pods were treated with NBT. (Jabs et al, 1996) Pods treated with

1  $\mu$ M bruchin or a control were submerged in 0.1% NBT in 10 mM  $\text{KH}_2\text{PO}_4$  buffer for 30 min and evaluated microscopically. Mechanical wounding acted as a positive control.

## TUNEL

TUNEL Kit DeadEnd™ Fluorometric TUNEL system (Promega Cat.#G3250) was used on paraffin embedded tissues. The TUNEL (TdT-mediated dUTP Nick-End Labeling) assay enzymatically incorporate fluorescein-12-dUTP to 3'-OH DNA ends with terminal deoxynucleotidyl transferase (TdT) forming a fluorescent polymeric tail. The fluorescein-dUTD could be visualized with a FITC filter set at  $520 \pm 20$  nm using a fluorescent microscope. Propidium iodide was used as a counter stain, emission 620 nm (Sigma. Cat.# P4170), and to sustain dye fluorescence Molecular Probes SlowFade Kit (S-7461) was used. Promega kit instructions were followed for paraffin-embedded tissues except the concentration of the fluorescein-12-dUTP tag was reduced by 5X as per Klosterman, et al. (2000). The TUNEL assay was repeated two times.

## Propidium iodide

3, 8-Diamino-5-(3-diethylmethylamino)propyl)-6-phenyl phenanthridinium diiodide; propidium iodide (PI)(Sigma Cat.#P4170) is a dye specific to double stranded nucleic acid with excitation 493 nm and emission 630 nm.

## Evans Blue

Evans Blue (EB)(Sigma Cat.#46160) (also known as Direct Blue 53) enters cells with a freely permeable plasma membrane, and this serves as an assay for cell death.

Entire pods were submerged for 3 min in 2% EB in water. The pods were rinsed in H<sub>2</sub>O and viewed microscopically.

#### Rose Bengal

Rose Bengal (RB) (Sigma Cat.#R3877) (excitation Abs 556 nm emission 572 nm in MeOH) was used as generated of singlet oxygen. On two sets of *Np* and two sets of *np* pods, grown outside, and two sets of each type grown in the greenhouse 1  $\mu$ L of RB at 40 mM, 4 mM, 400  $\mu$ M, 40  $\mu$ M and 4  $\mu$ M were applied to pods. One pod in each set was covered with foil for 24 h following treatment with RB to control possible photobleaching. The pods remained on the plants until harvested and evaluated after 5-7 days.

#### Diphenylene iodonium chloride (DPI)

A diphenylene iodonium chloride (DPI) (Sigma Cat.#02926) stock solution of 2.5 mM in 50% ethanol was stored at -20 C and diluted to 1 mM, 100  $\mu$ M or 10  $\mu$ M as needed. Pods grown in +UV were treated with 1  $\mu$ L of each DPI concentration, allowed to dry, and then 1  $\mu$ L of 1  $\mu$ M bruchin was applied. Pods were allowed to develop 5-7 days and then neoplasm growth was evaluated. For SN the pods grown in the greenhouse were treated by spreading 8  $\mu$ L of each concentration of DPI across the entire surface of one side of the pod or spot treated. These pods were grown until neoplasm occurred on the untreated control (typically in 5 to 7 days) and SN on pods were compared.

#### DAPI

A 100  $\mu$ M stock solution of 4', 6'-diamidion-2-phenylindole dihydrochloride (DAPI)(Molecular Probes D-1306) with excitation 358 nm and emission 461 nm was prepared in H<sub>2</sub>O. For experiments, stock was diluted to 300 nM with 1 X PBS.

Epidermal peels or cross sections of pods were placed in wells, floated in 20-50  $\mu$ L of 300 nM DAPI for 1 min and viewed microscopically.

Table 1 Compounds tested on *Np* and *np* for inhibitory or stimulatory activity.

Compound	Activity	Treatment
Ascorbic acid	Free radical scavenger; reducing agent in enzymatic reactions catalysed by hydroxylases	10 mM
Curcumin	Natural phenolic; inhibits iNOS; antioxidant properties	10, 100 $\mu$ M
Catechin +/-	Antioxidant flavanoid, scavenger, inhibits lipid oxidation	10 $\mu$ M 10 mM
Rutin	Polyphenolic flavanoid antioxidant; NO scavenger; attenuates H <sub>2</sub> O <sub>2</sub> production	10, 100 $\mu$ M 10 mM
N-acetyl-L-cysteine (NALC)	Antioxidant; increases cellular pools of scavengers	10 $\mu$ M 1mM
Diethyl dithiocarbamic acid	NO spin-trapping reagent; inhibits NOS	10, 100 $\mu$ M, 1mM,
CGMP (guanosin 3'5'-cyclicmonophosphate)	Second messenger; intracellular mediator of extracellular signals such as NO	10, 100 $\mu$ M, 1mM
diphenylene iodium (DPI)	Inhibitor of NADPH oxidase in mammals	1mM
SNAP (S-nitroso-N-acetyl penicillamine)	Nitric oxide (NO) donor; activates guanylate cyclase. Substitute for glutathione. Implicated in induction and prevention of apoptosis.	500 $\mu$ M
GSNO (S-Nitrosoglutathione)	Nitric oxide (NO) donor	500 $\mu$ M
Hydrogen peroxide (H <sub>2</sub> O <sub>2</sub> )	ROS and possible signaling molecule. Concentration and duration determines effect.	1, 5, 25 mM
Jasmonic acid (JA)	Regulates defense gene expression. Inhibits cAPX. An ROS scavenger	1, 10, 100 $\mu$ M, 1mM
Paraquat	Peroxide producer	10,100 $\mu$ M, 1mM
Aminotriazole	Superoxide producer	10,100 $\mu$ M, 1mM,
Rose Bengal	Singlet Oxygen producer; photosensitive	4, 40, 400 $\mu$ M 4, 40 mM,
A23187	Calcium ionophore very selective for Ca <sup>+2</sup> Stimulates NO production.	100, 250 $\mu$ M
Salicylic acid (SA) (2-hydroxybenzoic acid)	Involved in the up regulation of defense genes and SAR. Inhibits JA; can inhibit or enhance Ca <sup>+2</sup> and apoptosis.	25, 250 $\mu$ M
Genistein (4,5,7-trihydroxyisoflavone)	ATP-binding site competitor inhibits kinases but major inhibition of protein tyrosine kinases	1, 10, 100 $\mu$ M, 1mM
Bay le 8644 R(+), S(-)	Acts on slow Ca <sup>+2</sup> channels; S(-) blocks and R(+) activates Ca <sup>+2</sup> channels	25, 250 $\mu$ M
Fumonisin	Fungal toxin; known to trigger apoptosis and cell division, blocks formation of ceramide.	70, 700 $\mu$ M

all compounds were ordered from Sigma

Compounds were mixed according to manufacture recommendations to concentrations indicated.

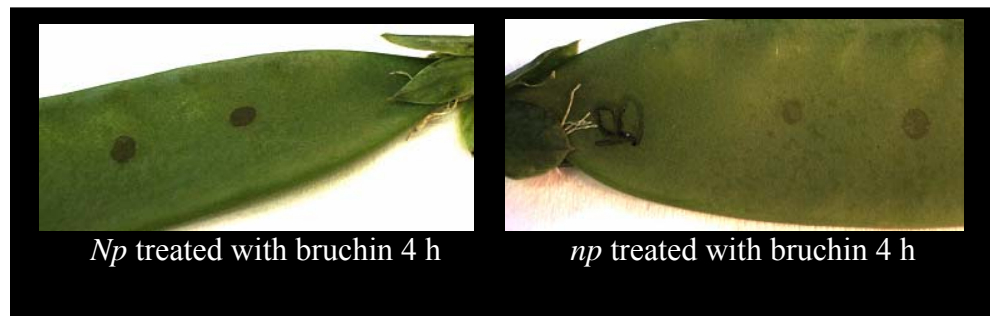
## Results

### 1. Bruchin

#### Browning and Fluorescence

Treating *Np* pods with bruchin initially produced browning (Fig. 5), followed by neoplastic growth at the application site (Fig. 4). The browning appeared to be cell death of the epidermal layer and was microscopically evident as little as 1 h after application. In these brown areas, cells collapsed within 24 h (Fig. 6 a,e). In contrast to the rapid, clear response of *Np* pods, the browning response of *np* pods was much weaker (Fig. 5).

Fig. 5 Bruchin treatment of *Np* and *np* pods

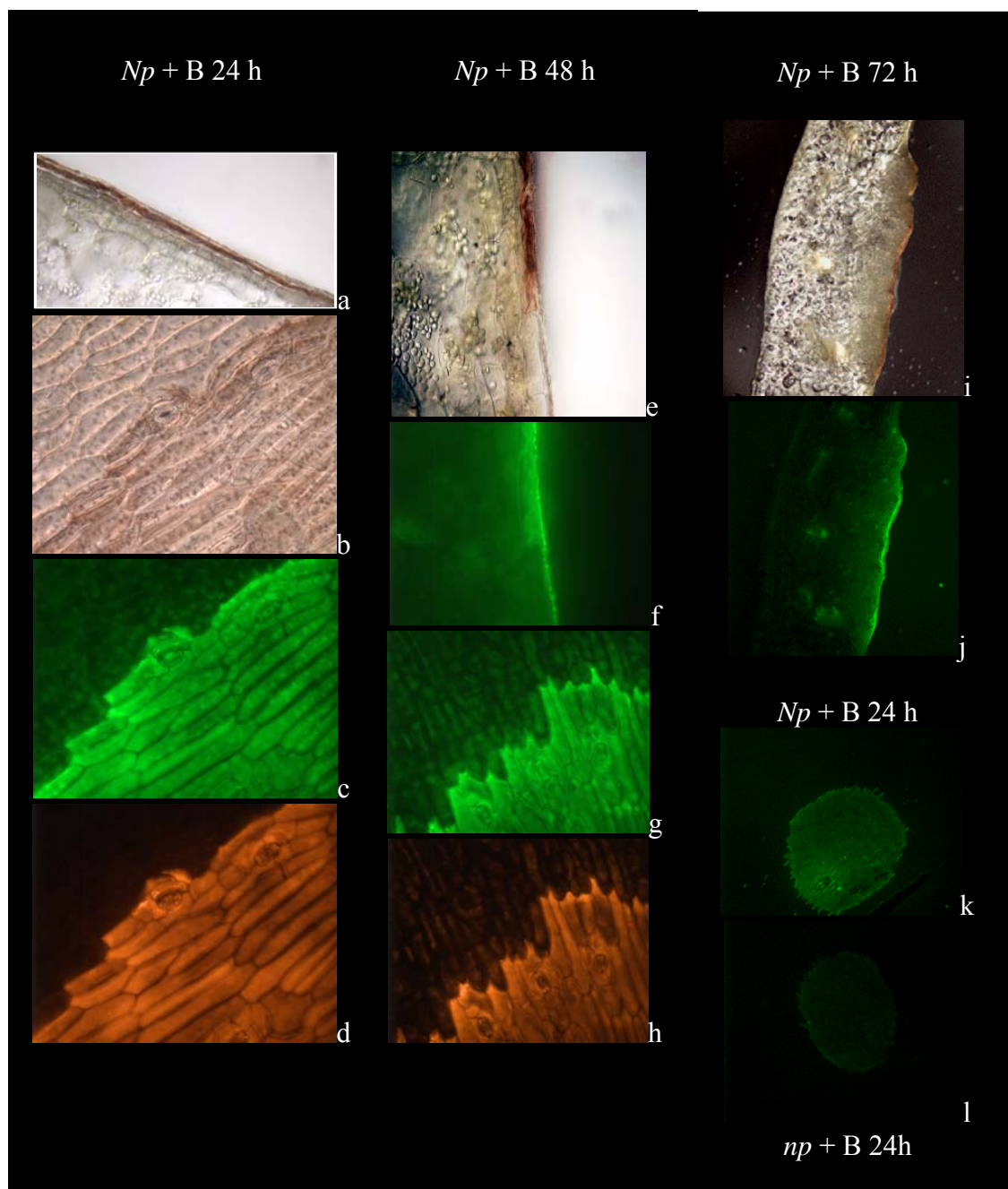


In addition to browning, bruchin-treated cells fluoresced. By 24 h after treatment, the entire treated site fluoresced almost uniformly (Fig. 6 b-d). Both browning and fluorescence affected entire cells in the treated areas (Fig. 6 b-d, e-h, k); cells either responded to bruchin with browning and fluorescence or they did not. Fluorescence at 48 h was more intense, but there was no indication of cell division at this time (Fig. 6 f-h). By 72 h after treatment, neoplasm development was clearly evident at treated sites, with

Fig. 6 Browning and fluorescence of pod tissues.

Bruchin treatment with 1 $\mu$ M is indicated with B and +UV indicates full spectrum of light was used to grow the plants. (a-d) *Np* +UV + B 24 h. (a) *Np* pod with brown layer of collapsed epidermal cells. (b) Browning followed the parameter of cells. (c-d) Auto-fluorescence 24 h after bruchin treatment. (e-h) *Np* +UV + B 48 h. (e) 48 h after bruchin treatment the epidermis was collapsed and (f) increased auto fluorescence was confined to the treated epidermal layer. There was fluorescence of pod surface wax. (g-h) Auto-fluorescence 48 h after B treatment. (i-j) *Np* +UV + B 72 h neoplasm development was clear. The brown and fluorescent epidermal layer 'floats' above the mounded calli. (k-l) Comparison of epidermis of *Np* and *np* +UV + B 24 h. (k) *Np* +UV + B 24 h and (l) *np* +UV + B 24h. Fluorescence of *np* pod was considerably less than the fluorescence of the *Np* pod.

Fig. 6 Browning and fluorescence of pod tissues.



the epidermal cells continuing to fluoresce at the upper surface of the neoplasm (Fig. 6 i-j). Pods of *np* were not as fluorescent as *Np*, compare Fig. 6 k (*Np*) to Fig. 6 l (*np*).

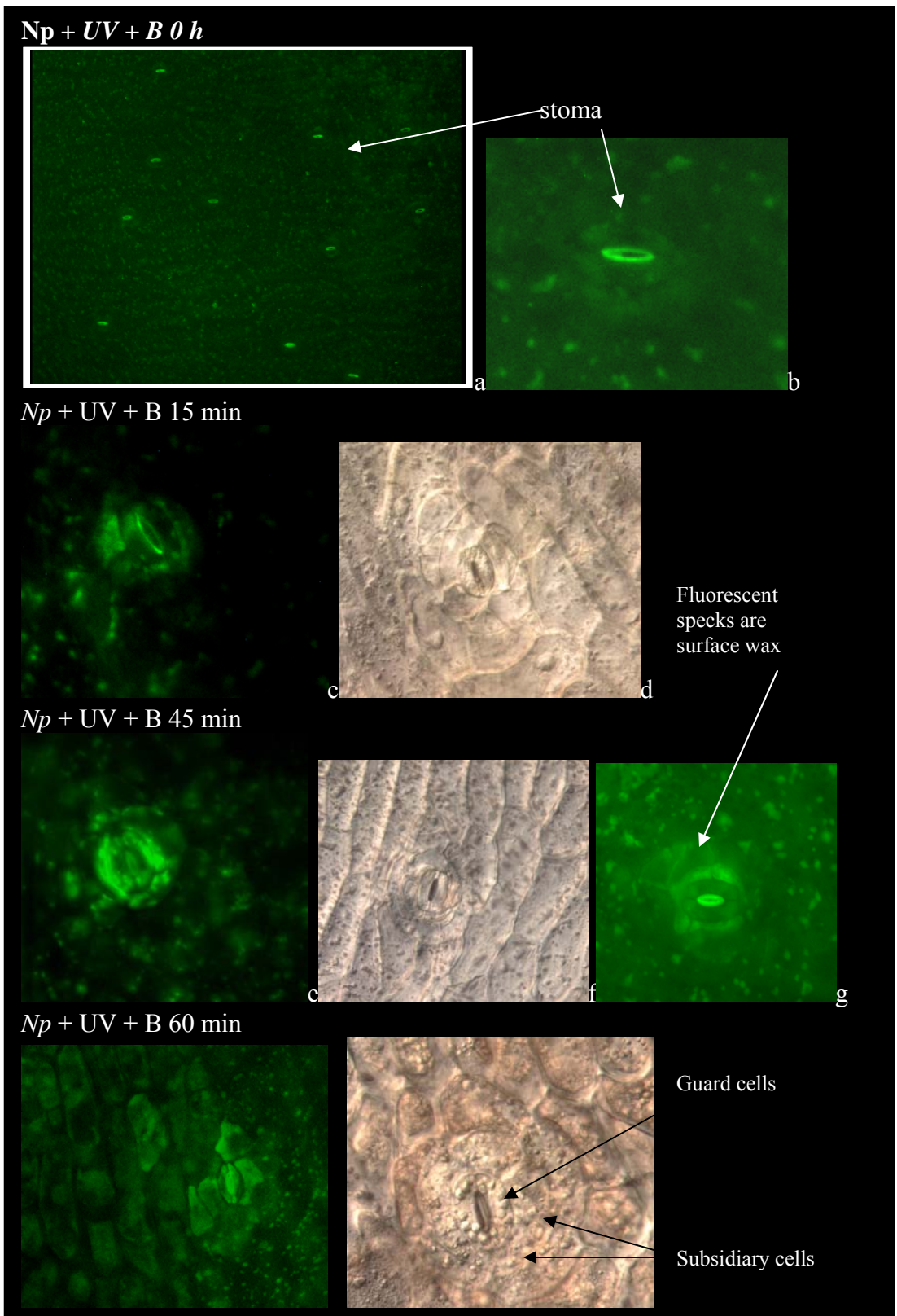
These bruchin-induced events required an intact pod or sections with all pod cell layers intact. Peeled epidermis and exposed mesophyll cells did not respond to bruchin with browning and fluorescence. Treating intact pods with bruchin and then peeling the epidermis at any time stopped the response. Even though peeled cells were unresponsive to bruchin, cytoplasmic streaming was still evident indicating the cells were still alive. Therefore, development of the bruchin response was initiated by treating intact pods and peeling the epidermis at various times to investigate further the effect of bruchin on epidermal cells.

Prior to bruchin treatment, a small percentage of the stomata on outdoor-grown *Np* pods (*Np* +UV) fluoresced at the interior surface of the guard cells that form the stoma (Fig. 7 a, b). Within 15 min after bruchin treatment, fluorescence increased and included the guard cells as well as the extracellular space between the guard cells and the subsidiary cells (Fig. 7 c). Subsidiary complex cells exhibited no intracellular changes at this point (Fig. 7 d). However by 45 min after treatment, the entire stomatal complex was intensely fluorescent (Fig. 7 e, g). Increased fluorescence was accompanied by development of dense grainy appearance in the subsidiary cells (Fig. 7 f). At 1 h, it appeared the fluorescence had begun spreading to adjacent epidermal cells, though the stomatal complex remained the brightest area (Fig. 7 h). Browning of the epidermis had developed at this time and was evident in light microscopy (Fig. 7 i). In contrast to *Np*, fluorescence of *np* pods did not change appreciably during the first hour after treatment with bruchin.

Fig. 7 Development of fluorescence following bruchin treatment of pods.

Growing pods outdoors suppresses SN development. Pods grown outdoors are indicated with +UV. (a-b) *Np* +UV + B 0 h. Pods had moderate fluorescence evident at the stoma. Wax on the pod surface auto-fluoresced. (c-d) *Np* +UV + B 15 min. (c) guard cells fluoresce; the intracellular space between the guard cells and the subsidiary cell and the subsidiary cells themselves were fluorescent. (d) Using light microscopy the subsidiary cells did not appear changed. (e-g) *Np* +UV + B 45 min. fluorescence was greater and light microscopy revealed changes in the subsidiary cells. Each stomatal complex reacts individually and complexes right next to each other had variable degrees of response (note the differences in e and g). (h-i) *Np* +UV + B 60 min. (h) The stomatal complex was brilliantly fluorescent, the epidermal cell were also beginning to fluorescence. (i) Light microscopy showed clear changes in the subsidiary cells and browning was evident across the epidermal surface.

Fig. 7 Development of fluorescence following bruchin treatment of pods.



The response to oviposition mirrored the bruchin response. Eggs deposited on the *Np* pods occasionally developed browning that could be seen with the naked eye.

## ROS

As detected by DAB staining *Np* pods generated peroxide/peroxidase within 3 h of bruchin treatment (Fig. 8 a), and staining was most intense in epidermal cell nuclei (Fig. 8 b, c). Coinciding with peroxide development at the treatment site, the plasma membrane of stained epidermal cells pulled away from the cell wall (Fig. 8 c). By 24 h after bruchin treatment, DAB staining was detected along the epidermal surface a small distance beyond the treated site and into the mesophyll below the treated site (Fig. 8 e). In the mesophyll, DAB produced general staining (Fig. 8 e), but again, as with the epidermal cells, the nuclei stained most intensely (Fig. 8 f-h). In addition, chloroplasts clustered around the nuclei (Fig. 8 f-h). Bruchin treated *np* pods showed no DAB staining at 3 h (not shown) or at 24 h and no chloroplasts clustered around the nuclei (Fig. 8 d).

Tests for superoxide ( $O_2^-$ ) using NBT indicated that bruchin treatment did not result in  $O_2^-$  generation. Wounded pod tissues did stain, thereby providing a positive control for  $O_2^-$  assays (results not shown).

Exogenous application of hydrogen peroxide did not cause browning or cell division. Neither application of Paraquat® or aminotriazole, which are superoxide and peroxide producing agents, respectively, caused browning or cell division. However, Rose Bengal (RB), which generates singlet oxygen ( $^1O_2$ ), caused cell division at the site of application on greenhouse, but not outdoor grown (i.e. +UV) pods (Fig. 9 a, d). RB is

Fig. 8 DAB stain for H<sub>2</sub>O<sub>2</sub> in bruchin treated pods.

(a) *Np* +UV +B 3 h tissues indicated the presence of H<sub>2</sub>O<sub>2</sub> in the epidermal cells, and in the TE (tracheal elements), which were a positive control of a viable stain and method. (b) *Np* +UV + B 3 h nuclei in epidermal cells stained for the presence of H<sub>2</sub>O<sub>2</sub>. (c) *Np* +UV + B 3 h nuclear staining and cell shrinkage was evident. (d) *np* +UV + B 24 h; light staining of *np* tissues. (e) *Np* +UV + B 24 h peroxide staining was evident deep in the tissues. (f, g, h) *Np* +UV + B 24 h H<sub>2</sub>O<sub>2</sub> DAB stained nuclei in the mesophyll and cells below the treatment site. Bodies surrounding the stained nuclei were manifest in mesophyllic cells of *Np*. Neither nuclear peroxide staining nor vesicular bound bodies at the nucleus developed in *np*.

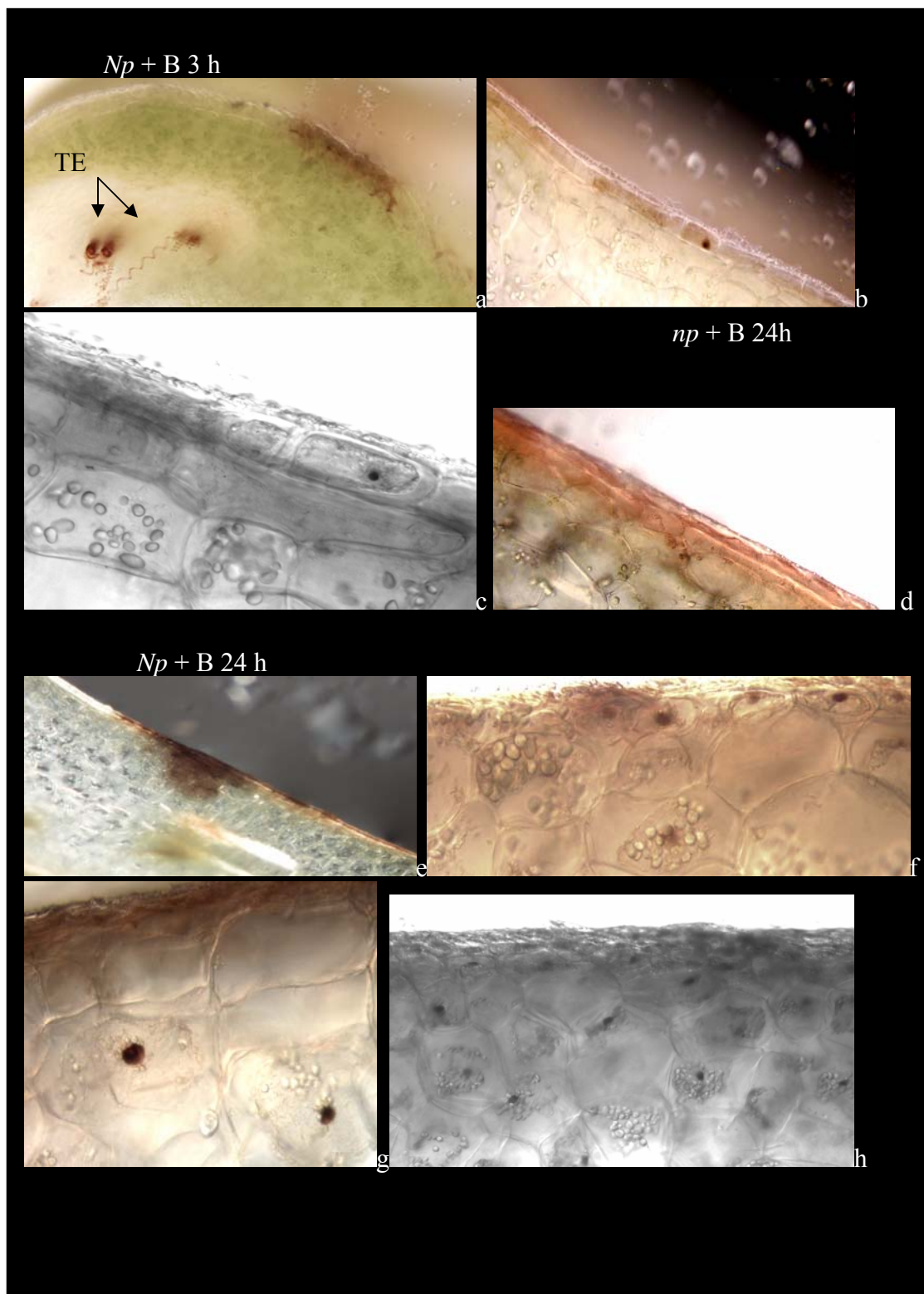
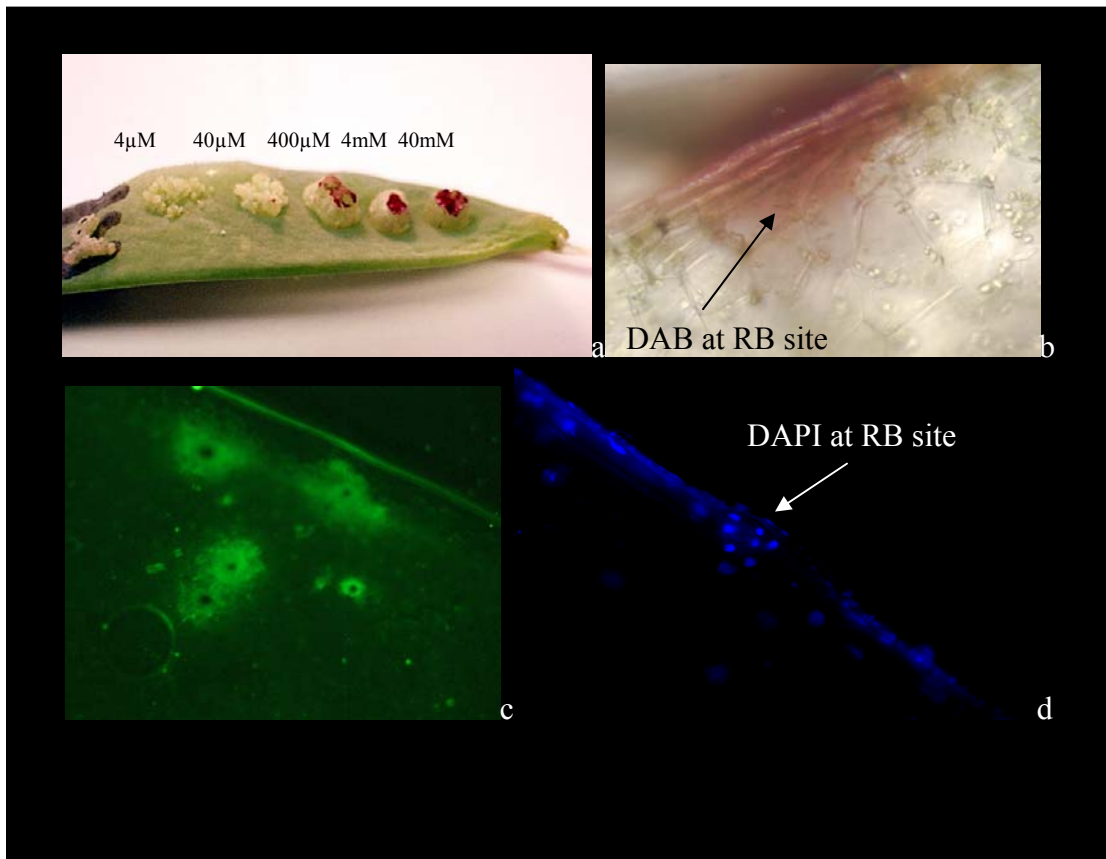
Fig. 8 DAB stain for H<sub>2</sub>O<sub>2</sub> in bruchin treated pods.

Fig. 9 Rose Bengal treated pod tissues.

(a) RB generated dose dependent neoplastic growth at the treatment site of pods grown in the greenhouse. (b) DAB staining indicated the presence of  $H_2O_2$ . (c) Auto-fluorescence developed at cells around the RB treated site and (d) DAPI indicates multiple nuclei under the RB treated sites.



a pigment whose presence prevented observation of browning but fluorescence was observed (Fig. 9c). DAB staining at these sites indicated the presence of peroxide in the epidermis and several cell layers into the mesophyll (Fig. 9 b). Interestingly, neoplasm also formed where Sharpie® markers were used to mark pods (Fig. 9 a).

Inhibitors of ROS formation were tested (Table 1). None of these compounds altered the bruchin response.

### Ca<sup>2+</sup> and Zn<sup>2+</sup>

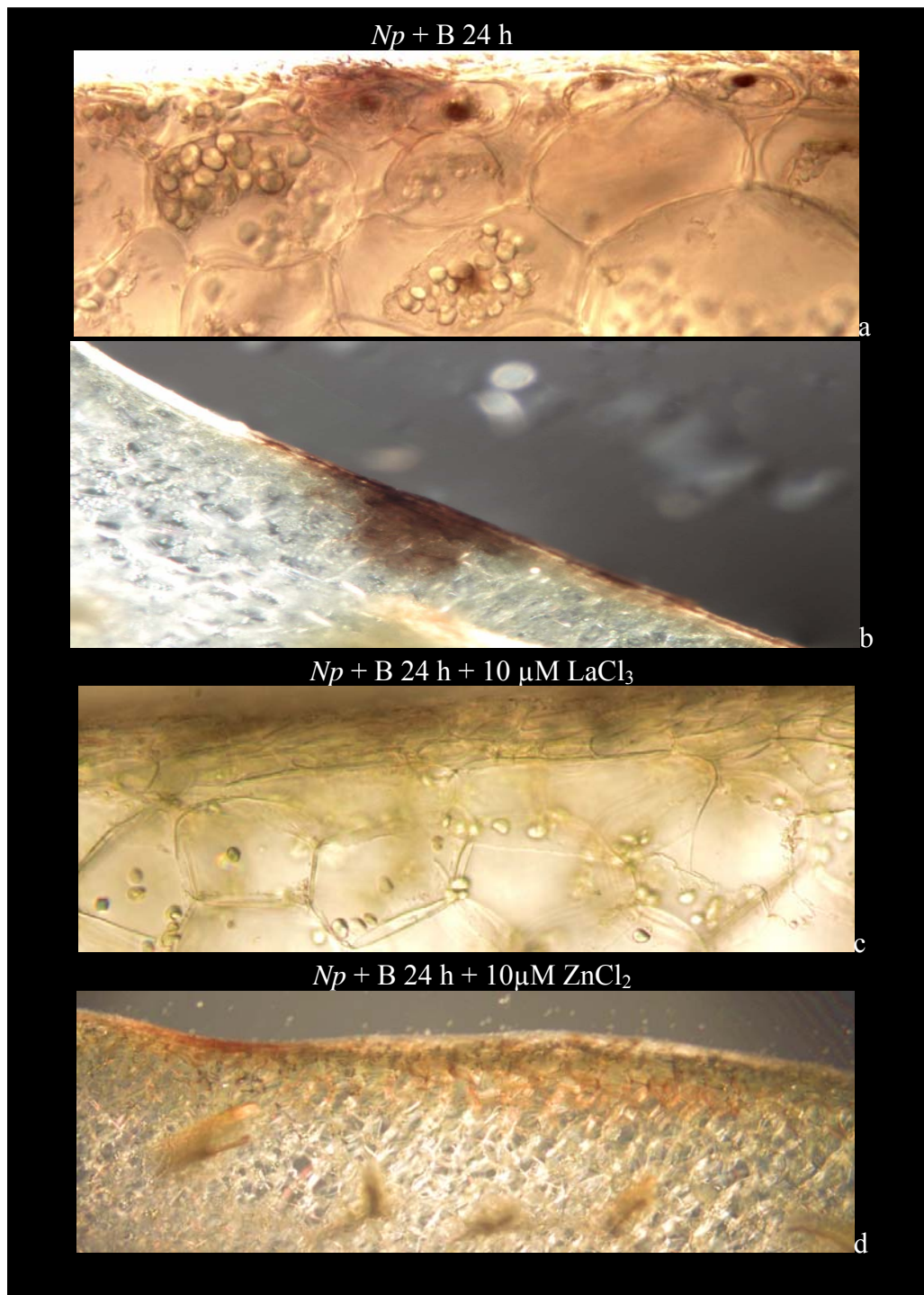
The role of Ca<sup>2+</sup> in bruchin-induced cell death was tested using several compounds that alter Ca<sup>2+</sup> flux A23187, a calcium ionophore; salicylic acid which can inhibit or enhance Ca<sup>2+</sup> concentration; Bayle 8644 R(+)/S(-) which acts on Ca<sup>2+</sup> channels; zinc and lanthanum a competitive inhibitors of Ca<sup>2+</sup> influx into cells. Application of 10 mM LaCl<sub>3</sub> prior to bruchin treatment prevented the development of neoplasm (W. Proebsting, unpublished results). Lanthanum also greatly reduced peroxide/peroxidase development, as indicated by the abolishment of DAB staining of the epidermal nuclei (compare Fig. 10 a,b with Fig. 10 c). Zinc chloride also inhibited the bruchin response. Cell division was significantly reduced, but not eliminated on pods treated with ZnCl<sub>2</sub> and then with bruchin. When assayed for peroxide/peroxidase, staining was reduced, but not eliminated, (Fig. 10 d). Other tested compounds failed to alter the bruchin response.

### TUNEL

Nuclear DNA (nDNA) fragmentation following bruchin or -UV treatment was assayed using TUNEL. In this assay, double-stranded DNA (dsDNA) in the cell

Fig. 10  $\text{LaCl}_3$  and  $\text{ZnCl}_2$  DAB stained for peroxide.

(a,b,c,d) *Np* +UV + B 24 h + DAB stain. (a, b) *Np* +UV + B 24 h indicated peroxide presence in nuclei and in tissues under the treatment site. (c) 10 mM  $\text{LaCl}_3$  inhibited peroxide development. (d) 10 mM  $\text{ZnCl}_2$  reduced peroxide development.



fluoresced red as a result of propidium iodide (PI) staining and any nicked DNA, with free 3' OH ends, fluoresced green as a consequence of enzymatic tagging with fluorescein-12. Where the two overlap, yellow fluorescence indicated the presence of dsDNA with free 3' OH ends.

The TUNEL control *Np* +UV + B 3 h without TdT enzyme, indicated the degree to which the fluorescent tag is inherently 'sticky'. Results showed no green fluorescein-12 tag indicative of nDNA nicking, but PI staining confirmed the presence of dsDNA (Fig. 11 a-c). *Np* +UV + B 3 h without the fluorescein-12 tag provided an indication of the degree of sample auto-fluorescence, which was minimal (Fig. 11 d). Propidium iodide stained nuclei as expected and the overlay shows no DNA nicking (Fig. 11 e-f). Use of *np* provided a biological control. Although *np* has a reduced bruchin reaction no fluorescein tagging was detected and the overlay showed no sign of DNA nicking (Fig. 11 g-i). DNase I-treatment of pod sections served as a positive control, demonstrating that nuclei do indeed label with fluorescein-12 when treated with nuclease (Fig. 11 j-k). Interestingly, the DNase I produced strong fluorescent labeling of the nuclei but the nuclei did not display the characteristic "eyeball" appearance evident with marginalization of the chromatin to the periphery of the nuclear envelope that develops in cells undergoing apoptosis. The DNase I nuclei do not look like the *Np* +UV + B 3 h complete (compare Fig. 11 j to Fig. 12 b).

At 1, 3 and 24 h following bruchin treatment, TUNEL detected progressive breakdown of DNA (Fig. 12 a-c). In as little as 1 h following bruchin treatment, there were signs of DNA nicking in nuclei of stomatal complex cells (Fig. 13 a-f). The nucleolus was evident with PI staining but chromatin did not appear to be nicked, as there

was little fluorescein-12 tagging. dsDNA appeared throughout the nuclei (Fig. 13 f). By 3 h after treatment, nicking greatly increased and was centered in cells of the stomatal complex (Fig. 14 a-c). Stomatal complexes visualized with confocal microscopy, displayed prominent nucleoli (Fig. 14 d-f) and chromatin demonstrated more fluorescence tagging of free 3' OH (compare Fig. 14 d to Fig. 13 b, d). By 24 h, bruchin-treated sites were heavily tagged, including some nuclei in the mesophyll directly below the treated epidermal cells (Fig. 15a-f). It appeared that the chromatin had marginalized, shifted away from the nucleolus, to the periphery of the nuclear membrane (Fig. 15 d-f). Overall auto-fluorescence of the epidermal surface had also increased (Fig. 15 a, c).

#### Transmission electron microscopy (TEM)

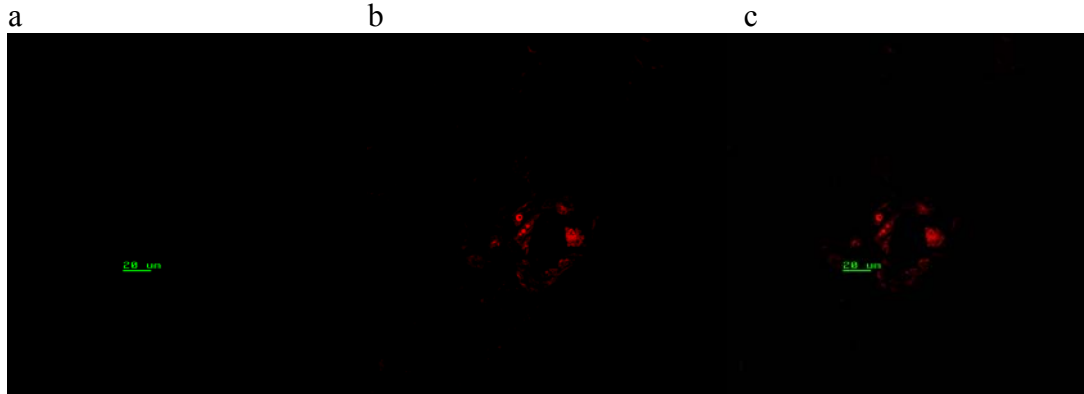
At zero time (Fig. 16 a-d) TEM examination of cellular contents revealed normal sized mitochondria (Fig. 16 c white arrow) and an unremarkable cytosol. Mitochondria swelling (Fig. 16 e white arrow) and a dense and grainy cytosol, indicating apoptosis, appeared in tissues one hour after bruchin treatment (Fig. 16 e-g). TEM revealed that by 4h post bruchin treatment nuclear blebbing (Fig. 16 h red arrows) as well as distended mitochondria (Fig. 16 i white arrow) were evident. Also at 4 h the cytosol of subsidiary cells was densely grainy with what appeared to be ribosomes free in the cytoplasm (Fig. 16 i). Prominent in the subsidiary cell cytoplasm were enlarged but intact mitochondria containing distorted cristae (Fig. 16 i).

Fig. 11 Controls for TUNEL assay of tissues treated with bruchin.

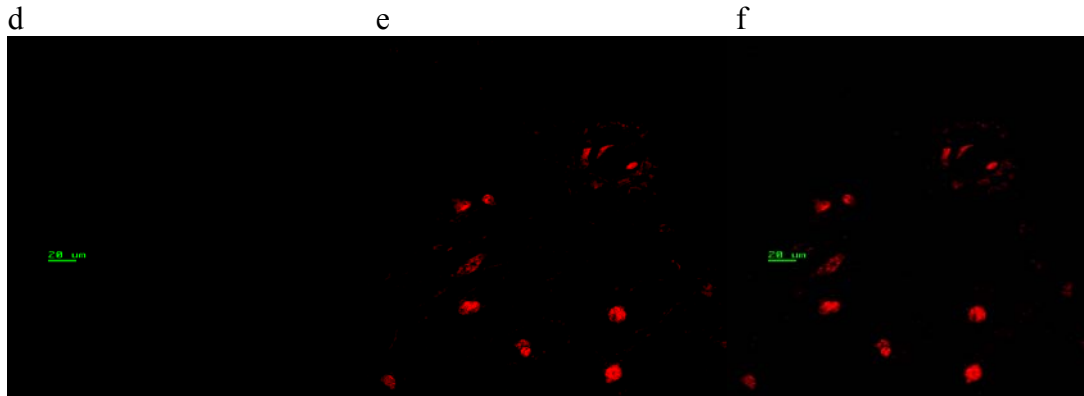
*Np* +UV + B 3h without enzyme was a negative control that (a, b,c) indicated the 'stickiness' of the tag without enzyme. (a) No green stain indicates there is no labeling of DNA. (b) Red indicates there is double strand DNA present. *Np* +UV + B 3 h without the tag. (d, e, f) enabled an assessment of the auto-fluorescence of tissues. *np* +UV + B 3 h with the complete TUNEL assay (g, h, i) was a biological control that allowed the determination of a limited response since the recessive does have some bruchin activity. (c) A yellow appearance would result from red fluorescent PI staining of dsDNA overlaid with green fluorescent stained nicked DNA. As a positive control *Np* +UV + B 0 h + DNase I (j, k) induced cleaving of DNA and showed that cleaved nDNA do light up when assayed with TUNEL.

Fig. 11 Controls for TUNEL assay of tissues treated with bruchin.

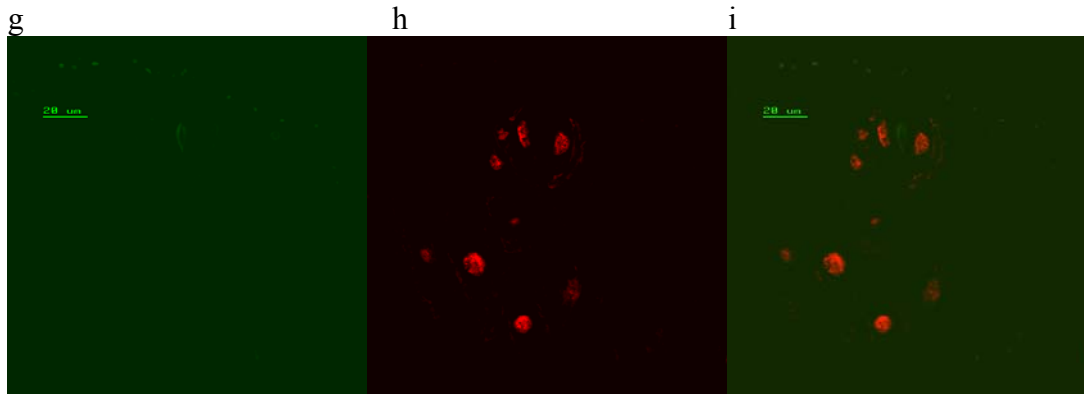
*Np* +UV +B 3 h no enzyme



*Np* +UV +B 3 h no tag



*np* +UV +B 3h complete



Positive control for TUNEL.

*Np* +UV +B 0 h Dnase I

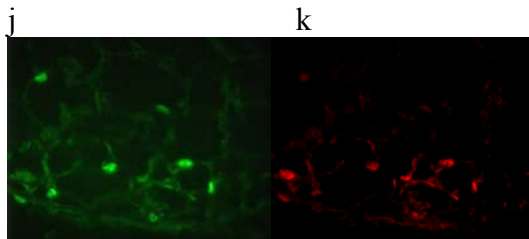


Fig. 12. Progressive development of nuclear degradation of tissues treated with bruchin.

(a) Green stain indicates labeling of 3'OH of nicked DNA. (b) Red indicates there is double strand DNA present. (c) Yellow resulted from red fluorescent PI staining of dsDNA overlaid with green fluorescent stained nicked DNA (a) *Np* +UV + B 1 h the nuclei had moderate fluorescent tagging of nicked DNA. (b) *Np* +UV + B 3 h tagging of nicked DNA is greater and the nucleolus is more prominent. (c) *Np* +UV + B 24 h there was more DNA nicking and the nucleolus appears larger with condensed and fragmented chromatin having moved to the parimeter of the nuclei.

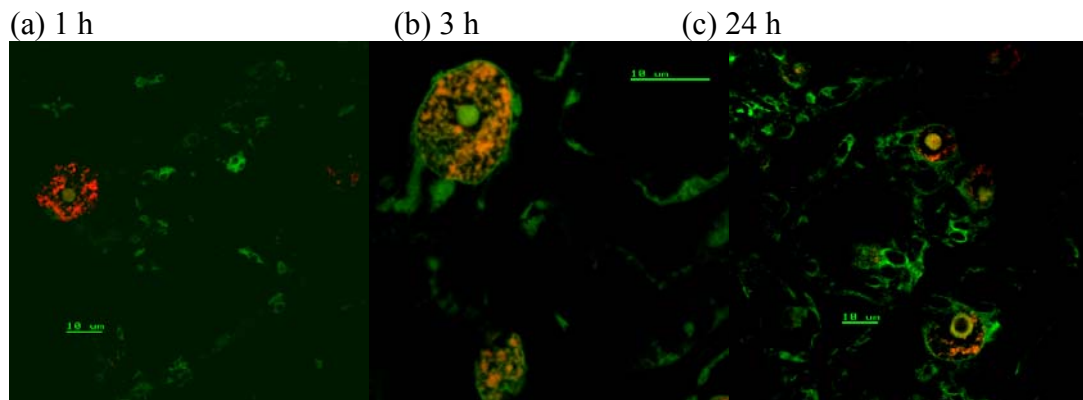


Fig. 13. Complete TUNEL of tissues treated with bruchin at 1 h.  
*Np* +UV + B 1 h complete

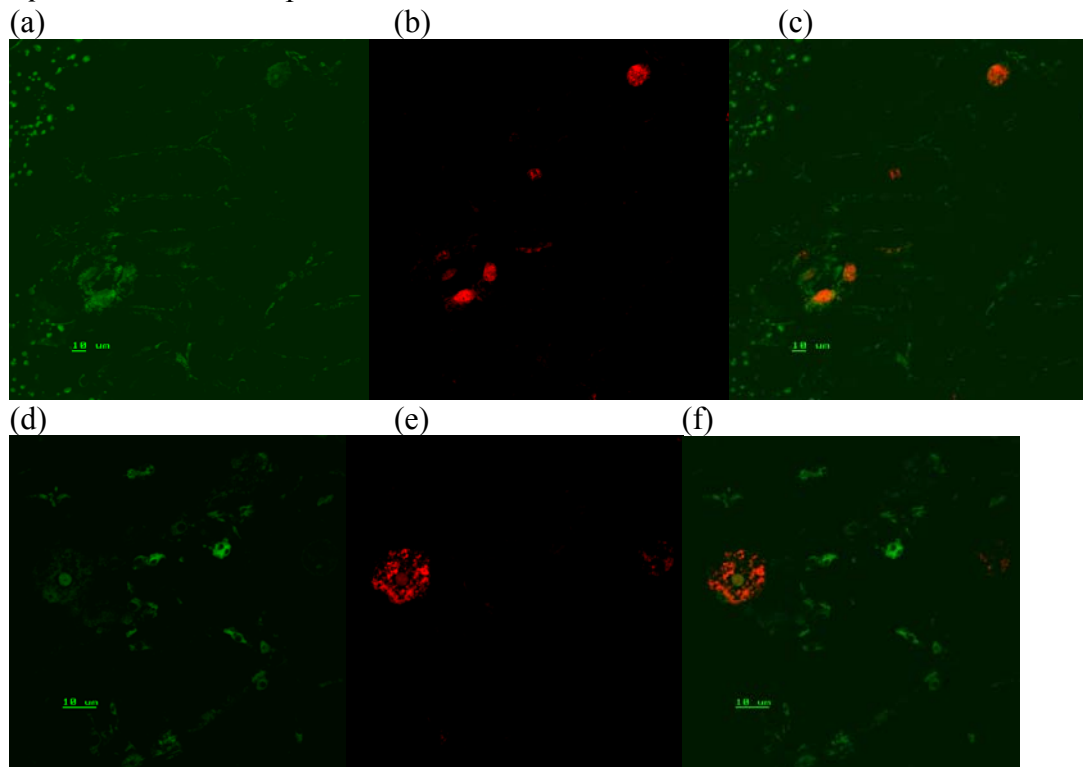


Fig. 14 Complete TUNEL of tissues treated with bruchin at 3 h.

(a) Green stain indicates labeling of 3'OH of nicked DNA. (b) Red indicates there is double strand DNA present. (c) Yellow resulted from red fluorescent PI staining of dsDNA overlaid with green fluorescent stained nicked DNA.

*Np* +UV + B 3 h complete

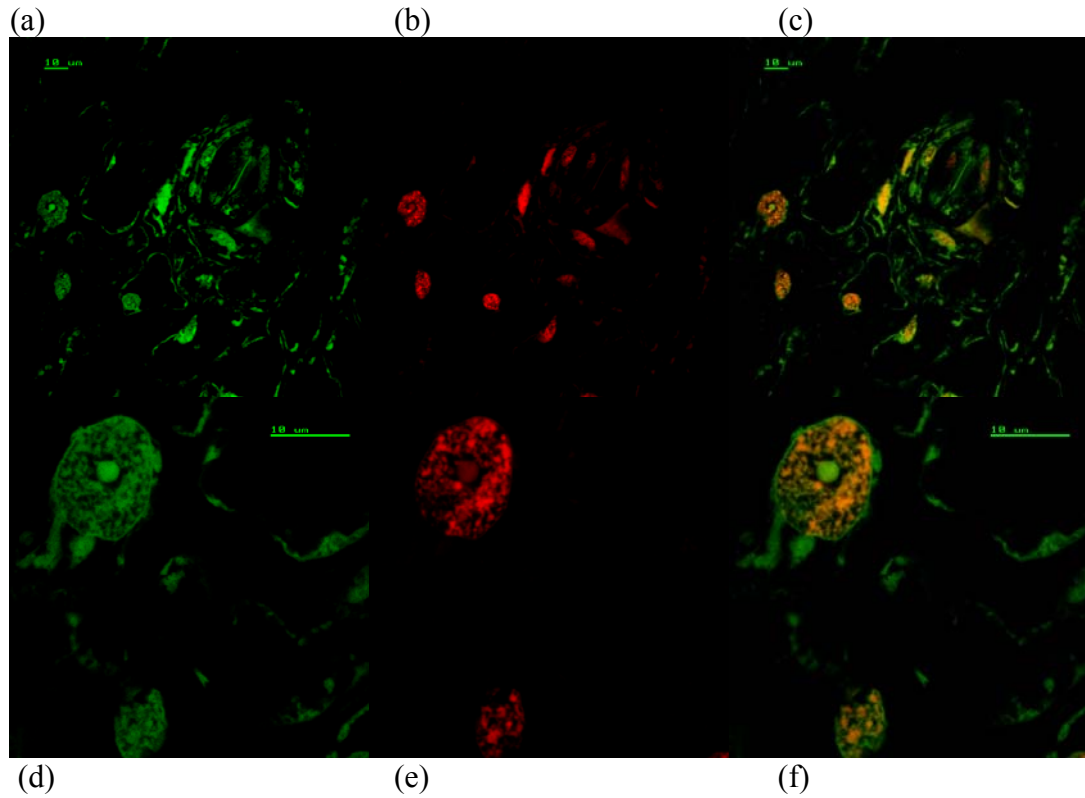


Fig. 15 Complete TUNEL of tissues treated with bruchin at 24 h.

(a) Green stain indicates labeling of 3'OH of nicked DNA. (b) Red indicates there is double strand DNA present. (c) Yellow resulted from red fluorescent PI staining of dsDNA overlaid with green fluorescent stained nicked DNA

*Np* +UV + B 24 h complete

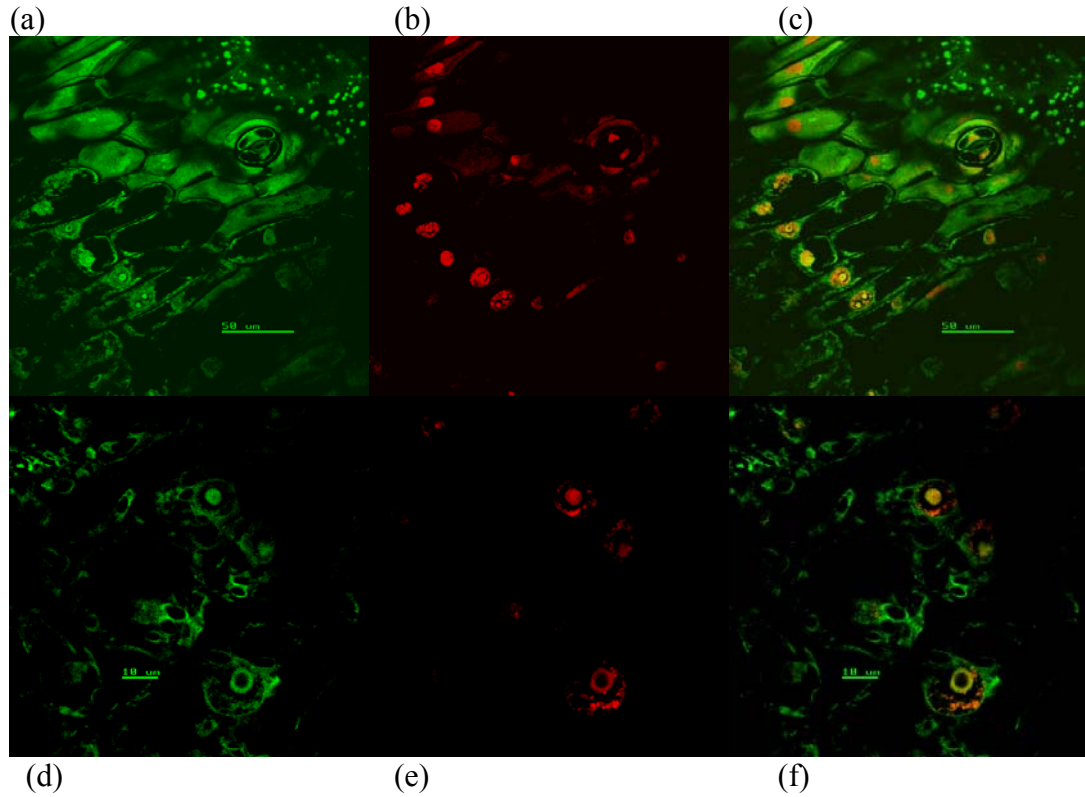
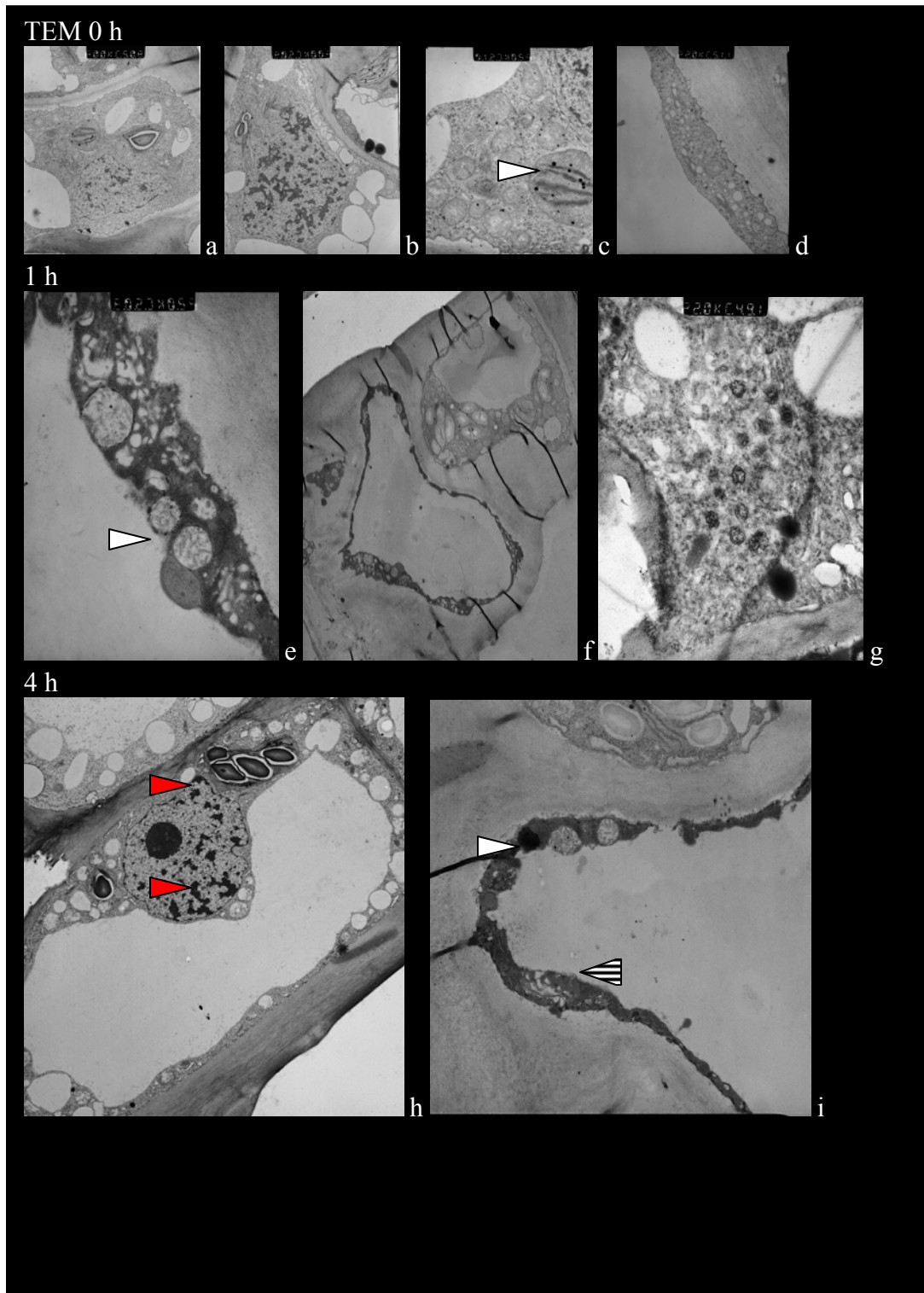


Fig. 16 TEM of pod tissues.

Tissues at time zero (a-d) show normal cell constitution such as (c) normal mitochondria (white arrow). After 1 h bruchin treated cells (e-g) demonstrated considerable increase in cytosol density and swollen mitochondria (e - white arrow). At 4 h after bruchin treatment cellular organelles demonstrated changes including nuclear blebbing (h - red arrows) and condensation of the cytosol. The subsidiary cell cytosol (i) at 4 h was grainy and dense (I - barred arrow), mitochondria were still intact and cristae were swollen and enlarged (i - white arrow).

Fig. 16 TEM of pod tissues.



## 2. Spontaneous Neoplasm

### Browning and Fluorescence

Initiation of spontaneous neoplasm (SN) on *Np* pods grown in the greenhouse (-UV) showed no clear indication of browning, in contrast to bruchin treatment. However, fluorescence was a useful marker for the development of SN and was concentrated at stomatal complexes where SN initiated (Fig. 17 a). After outdoor-grown (+UV) pods were shifted to -UV, fluorescence evident on the stoma-side of the guard cells (Fig. 7 a) expanded to include the entire stomatal complex, as well as some adjacent epidermal cells within 48 h -UV (Fig. 17 b-d). Appreciable amounts of SN had developed by 5-7 days. Fluorescence failed to develop at *np* stomatal complex under -UV treatments and neoplasm did not develop over the pod surface (not shown).

### ROS

Pods in +UV and -UV were assayed for peroxide formation using DAB. Under +UV a small portion of stomata tested positive for H<sub>2</sub>O<sub>2</sub> (Fig. 18 a). Under -UV conditions, the first area to stain with DAB was the inner wall of the guard cell (Fig. 18 d). After 24 h of -UV, peroxide/peroxidase staining of stomatal complexes dramatically increased (Fig. 18 b). Eventually, staining encompassed the entire stomatal complex, moving from guard cells to the intercellular space between the subsidiary cells, then to the subsidiary cells, then the entire stomatal complex, and finally weakly over the pod surface (Fig. 18 c). It proved problematic to assay for DAB of epidermal and mesophyll nuclei as the pods in the greenhouse that were developing SN were mushy and difficult to

Fig. 17 Fluorescence development on pods bruchin treated and in -UV.

A comparison of (a) *Np* + 1  $\mu$ M bruchin treatment after 12 h on the right side and -UV spontaneous calli on the left indicated the robustness of the fluorescence development with each treatment. Fluorescent development at the stomatal complex of (b,c,d) *Np* -UV 48 h.

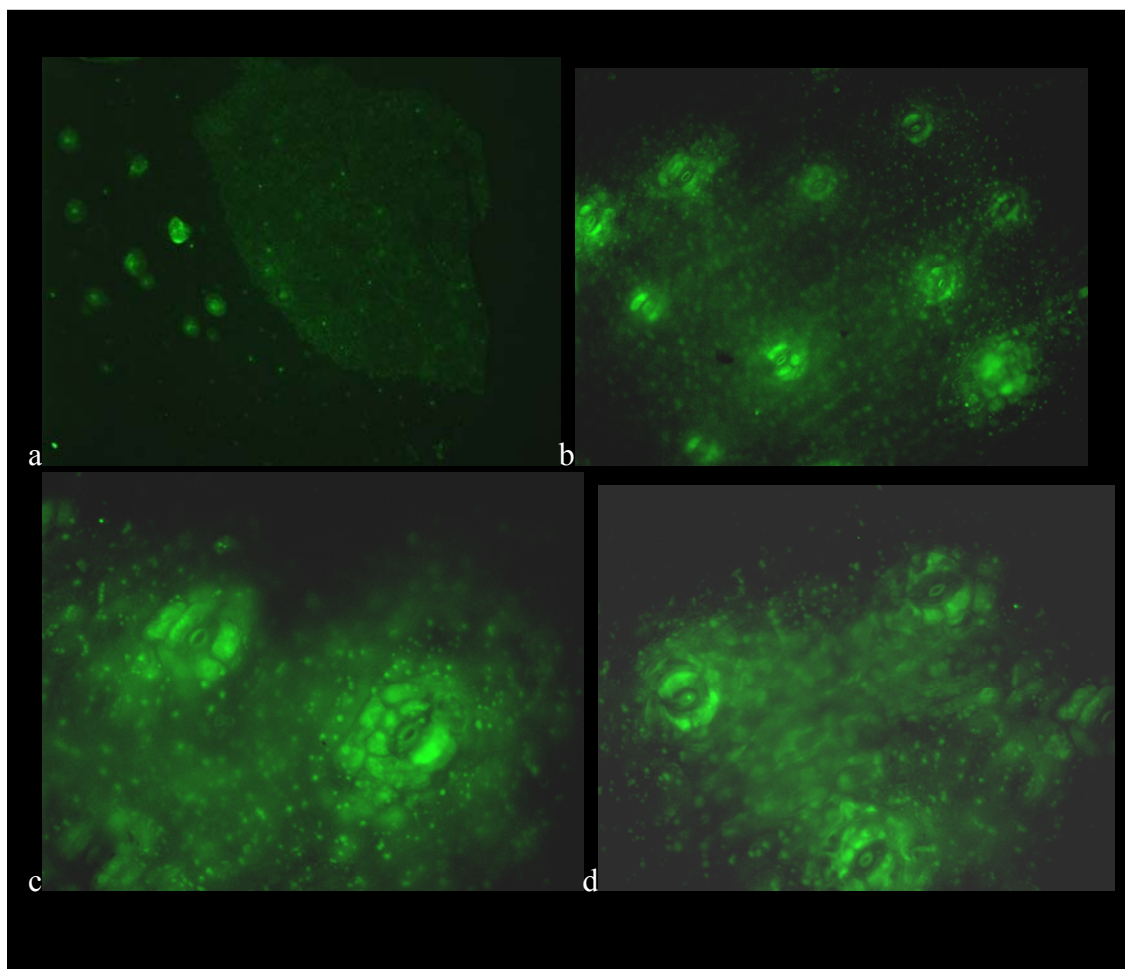
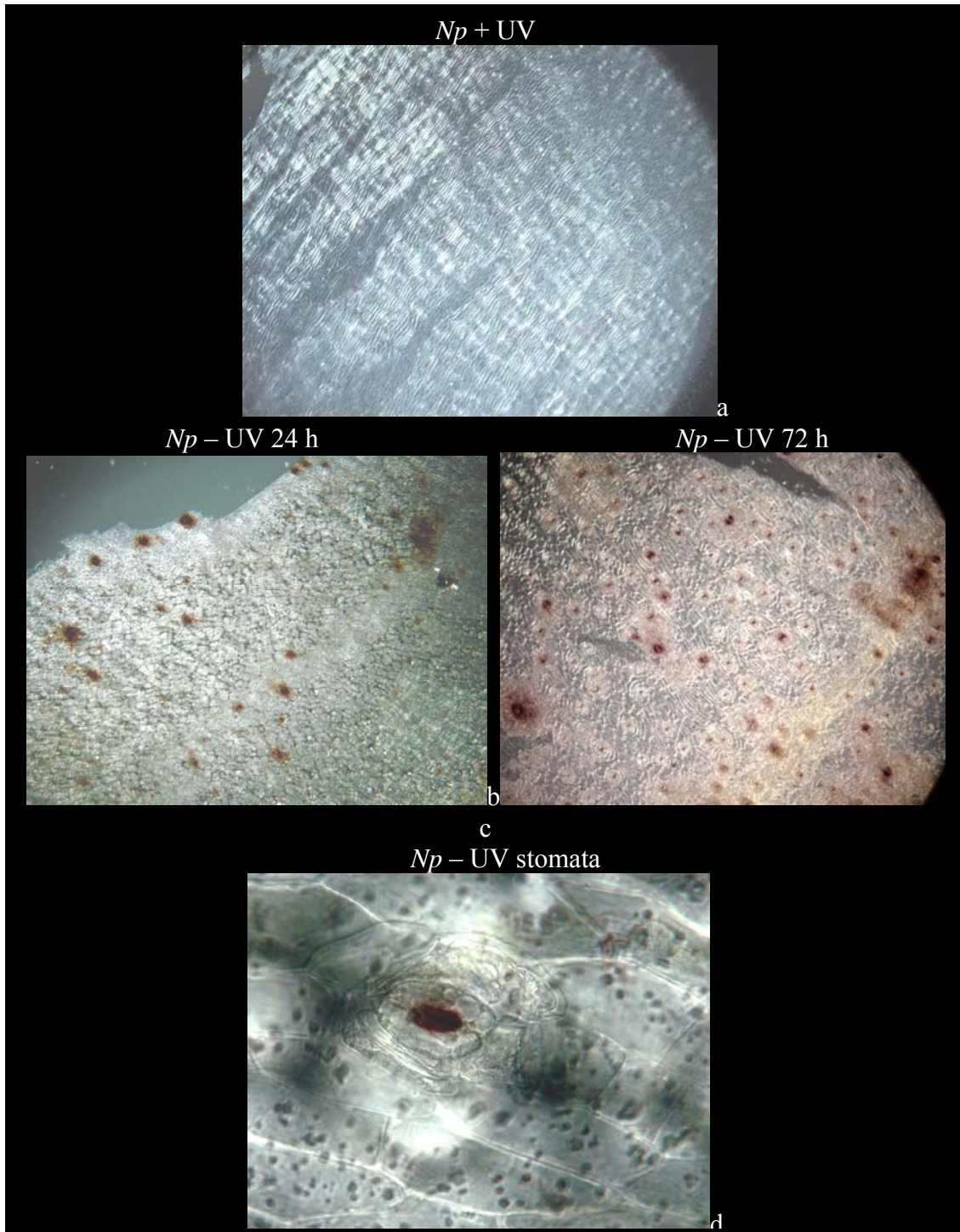


Fig. 18 Pods in -UV demonstrated progressively increased the amounts of peroxide staining of epidermal cells.

The first area on -UVtreated pods to stain for peroxide was the stomata complex. (a) *Np* +UV stained with DAB. (b) *Np* -UV 24 h stained with DAB at stomatal complex. (c) *Np* -UV 72 h stained with DAB (d).



section or were so heavily stained that nuclei were obscured. There was no increase in DAB staining associated with the *np* -UV treated pods.

#### TUNEL

TUNEL of pods treated with -UV for 48 h produced labeling comparable to bruchin treated pods. *Np* in -UV had DNA nicking that was most evident at the stomatal complex (Fig. 19 a-c) and evidence of DNA nicking increased as the time in reduced UV increased (data not shown). This change culminated in condensed and marginalized DNA at the perimeter of the nuclear envelopes similar to that of 24h bruchin treated samples (compare Fig. 19c to 14).

#### Evans Blue

Evans blue (EB) stain was used to search for evidence of cell death on pods in response to UV conditions or bruchin. In -UV light, EB progressively stained stomatal complex cells over the treatment period (-UV 0-72 h). Pods treated with -UV 24 h developed moderate EB staining at stomatal complexes (Fig. 20 d-e). Initially, staining was at the subsidiary cells with each complex reacting individually. This was observed in cross-sections of tissues (Fig. 20 f, j). Cells at the distal end of the pod developed neoplasm and EB staining first. By 48 h -UV staining was still predominantly around the stomatal complex (Fig. 20 f-g) and transverse sections of tissues revealed membrane bound bodies filling the cellular space of the epidermis (Fig. 20 h). Staining at 72 h -UV involved epidermal cells adjacent to the stomatal complex but was still most strongly expressed at the complex (Fig. 20 j-k). No EB staining was evident on *Np* +UV (0 h), or

*np* +/-UV (Fig.20 a-b). There was no EB staining of stomatal complexes on pod tissues in response to bruchin application (not shown).

Tracking changes in DAB and EB staining during SN development shows progressive increase in the concentration of ROS and compromised plasma membrane (indicated with EB) in the epidermis especially at stomatal complex sites on *Np* pod (Fig. 21).

A variety of compounds were tested on *Np* and *np* pods under low UV light conditions in an effort to affect PCD and/or mitosis. These compounds are listed in Table1. Jasmonic acid spot treated on *Np* -UV pods inhibited SN development. DPI (Fig. 22 a), which had no affect on bruchin treated pods inhibited SN development as did H<sub>2</sub>O<sub>2</sub>, Paraquat® and aminotriazole (Fig. 22 b-e). Further testing of these compounds has not been performed, thus limiting the ability to determine clear results.

Fig. 19 Complete TUNEL of tissues in -UV for 48 h.

(a) Green stain indicated free3'OH ends of nicked DNA. (b) Red staining indicated the presence of dsDNA. (c) Yellow color resulted when green and red panels are overlaid.  
*Np* -UV 48 h complete

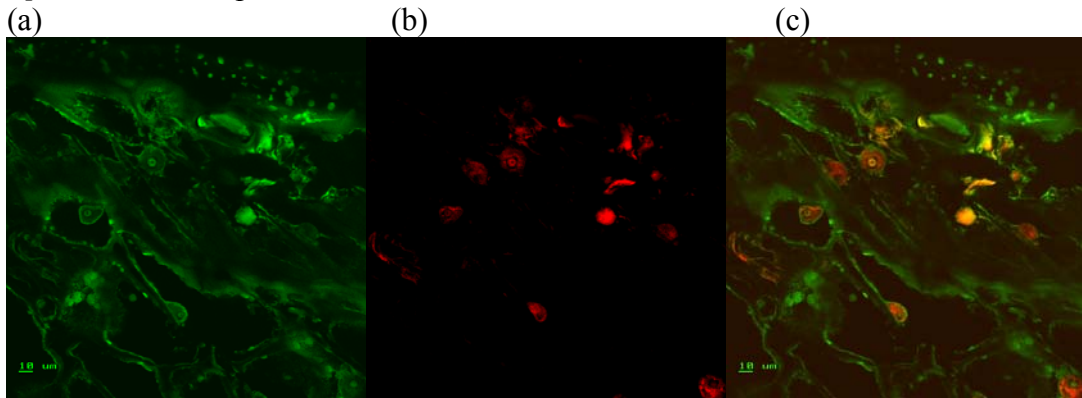


Fig. 20 Pods in -UV tested with EB indicated changing levels of PM integrity

(a) *Np* +UV did not stain with EB. (f) *np* +UV did not stain with EB. (c) *np* -UV 72 h showed no EB staining. But for (d-f) *Np* -UV 24 h there was an increase in EB staining with (e) each stomatal complex reacting individually. Complexes close to one another could demonstrate very different levels of staining. (f) Cross sections revealed EB stain concentrated at the stomatal complex. By (g-h) *Np* -UV 48 h. (h) there were membrane bound bodies visible in the epidermal and mesophyll cells and the PM was pulled away from the CW. (i-k) *Np* -UV 72 h showed a dramatic increase in EB staining and (j) cross sections showed strong staining at the stomatal complex.

Fig. 20 Pods in -UV tested with EB indicated changing levels of PM integrity.

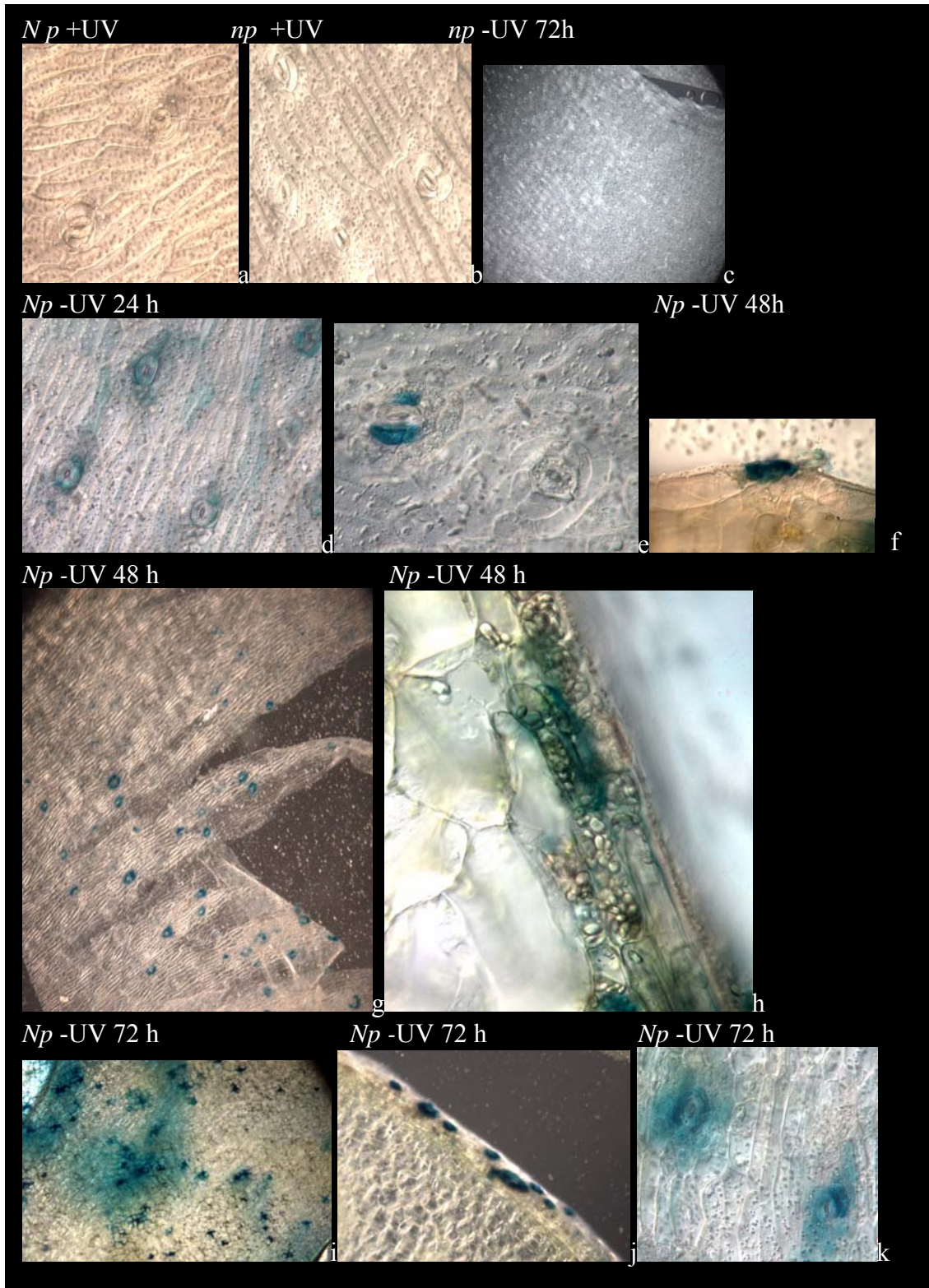


Fig. 21. A comparison of the percent of stomatal complex staining with DAB and EB indicated both increased over -UV treatment time.

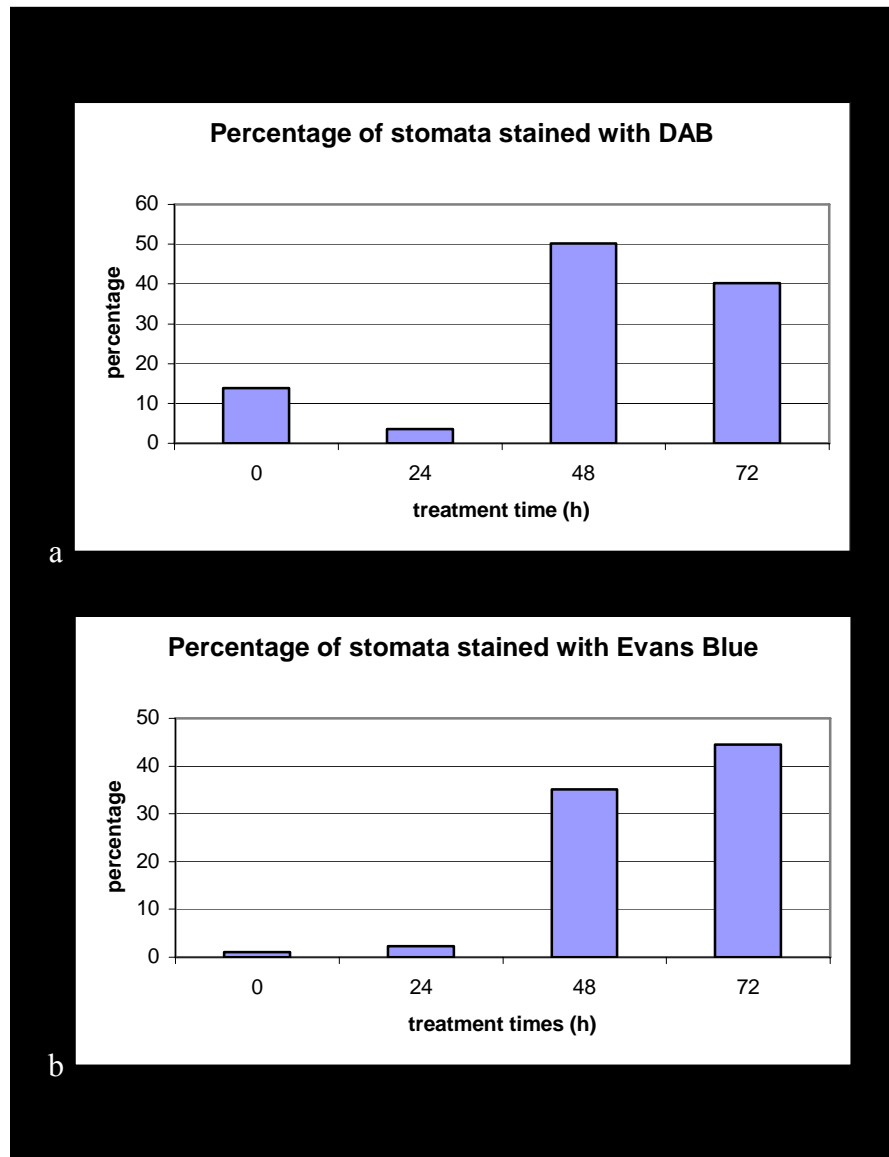
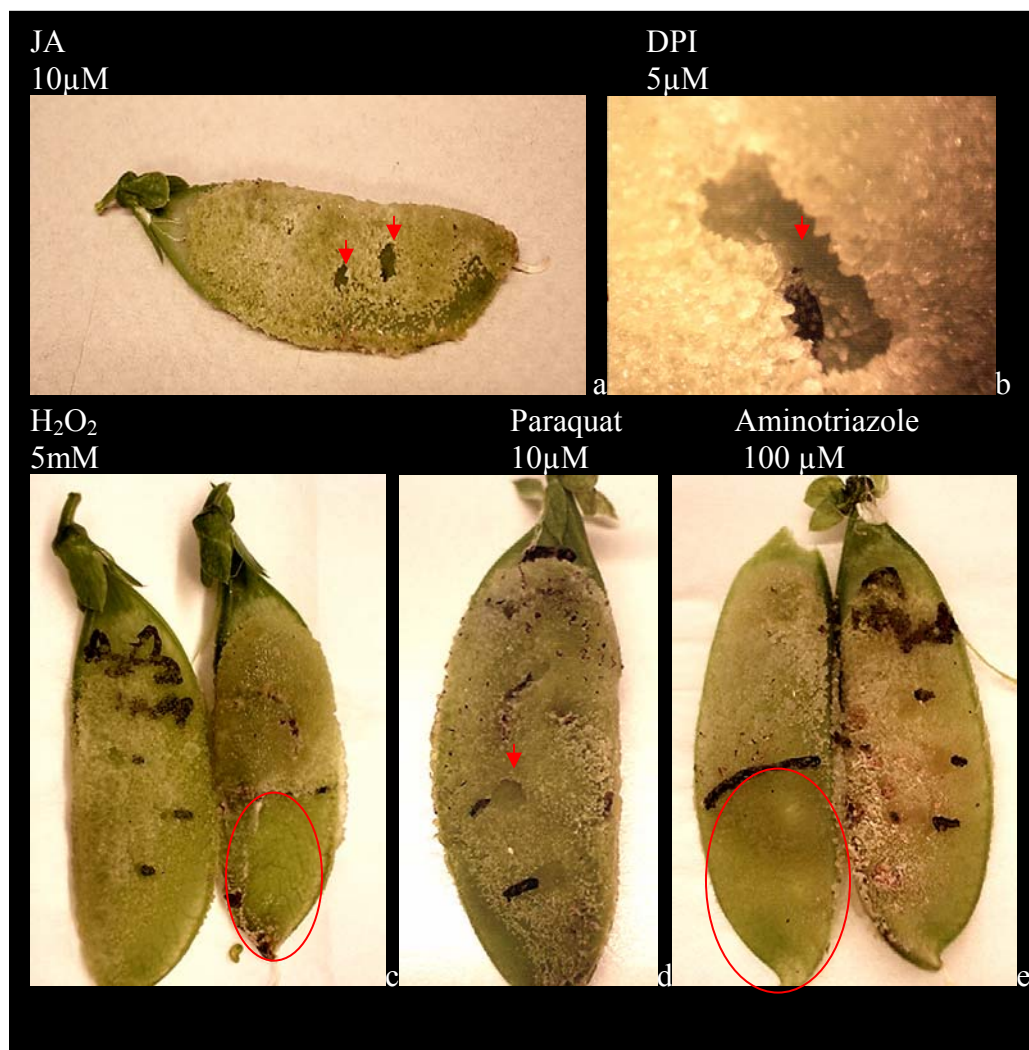


Fig. 22 Compounds inhibited the development of SN.

Compounds inhibited SN development in -UV was evident at 5-7 days. (a-e) *Np* pods were grown in -UV and treated as follows: (a) a pod spot treated with 10  $\mu\text{M}$  JA, (b) a pod spot treated with 5  $\mu\text{M}$  DPI, (c) a pod spot treated and an area smeared with 5 mM  $\text{H}_2\text{O}_2$ , (d) a pod spot treated with 10  $\mu\text{M}$  Paraquat®, (e) a pod spot treated and an area smeared with 100  $\mu\text{M}$  aminotriazole all showed inhibition of SN development.



## Discussion

Previous investigation revealed that the *Np* allele of pea conferred two phenotypes, which were expressed only on the pods. One, in response to an environmental cue, low UV light, produced spontaneous neoplasm (SN) which originated at the stomatal complex (SC). The second was a defense response to bruchid weevil oviposition, which triggers callus formation under the egg, pushing it away from the pod surface. The chemical that triggered the defense response was isolated and called bruchin. Bruchin mimics the oviposition response, stimulating neoplasm formation only at the treated site. Results presented here reveal that SN and the bruchin responses share common cellular characteristic : requirement for an intact pod, increased auto-fluorescence, production of ROS, apoptosis or PCD of epidermal cells, and neoplasm development

First, both phenotypes involved active cellular processes that required an intact pod. Neither epidermal peels, where cytoplasmic streaming was evidence of viability, nor exposed mesophyll cells responded to bruchin or -UV treatments. Second, auto-fluorescence was the initial response generated shortly after treatment and bruchin initiated response, which developed within minutes, was limited to the treatment site whereas -UV development of auto-fluorescence was slower and less specific.

Fluorescence developed consistently and rapidly at the bruchin treated areas prior to browning. Browning was previously observed and used to evaluate the bruchin activity of insect extracts (Doss et al, 2000). Bruchin induced auto-fluorescence began at the guard cells of the SC within 15 minutes and spread through out the treatment area within an hour. Auto-fluorescence did not spread beyond the site of treatment. *Np* in

-UV developed increased auto-fluorescence slowly, gradually, over the pod's surface beginning at the guard cells followed by stomatal complex cells and then epidermal cells. Plant auto-fluorescence responses have been demonstrated as a result of environmental cues such as UV and as a result of predation and pathogenesis (Fernandes 1990 Green and Fluhr 1995, Liakopoulos et al 2001 Sedlarova et al 2001). The waxy cuticle of plants contains phenolic compounds. The phenolic constituents of the guard cell's waxy layer may provide UV protection (Liakopoulos et al 2001). This cuticular layer absorbs shorter wavelengths of light affecting UV penetration to chloroplasts (Liakopoulos et al 2001 Sedlarova et al 2001). UV-B can trigger production of phenols and their subsequent deposition in the epicuticular wax layer resulting in increased auto fluorescence (Liakopoulos et al 2001 Sedlarova et al 2001). The -UV phenotype begins at the SC but engagement of the epidermal cells in the reaction does not begin for 24h.

My work showed for the first time that the bruchin response originates at the SC. In previously observations (Doss et al 1995), bruchin appeared to trigger a uniformed response in the treated epidermal cells. A closer look showed that guard cells responded in minutes with increased auto-fluorescence and the epidermal cells were engaged by 1h. Since the bruchin phenotype represents a defense response, any epidermal cell could have the ability to respond, as sensitivity of only a subset of surface cells to a pathogen or predator might unduly delay the defense response.

Generation of defense compounds and lignifications of the cell wall increases auto-fluorescence (Liakopoulos et al 2001, Sedlarova et al 2001, Alvarez et al 1998). Accumulation of phenolic compounds at sites of pathogenic penetration is a hallmark of HR (Fernandes 1990). Phenylpropanoids are normally made by cells and stored in the

vacuole (Sedlarova et al, 2001). These phenolic precursors are esterified by apoplastic peroxidases and incorporated into cell walls in the first stage of HR defense (Levine et al 1994). Subsequently, *de novo* synthesis of phenolic compounds and their accumulation on a wider scale prevent pathogen escape from HR (Sedlarova et al, 2001, Fernandes 1990).

Phenolic compounds esterified to surface wax can also be liberated during fungal hydrolytic processes and thereby limit hyphae growth (Liakopoulos et al, 2001). There is evidence that these liberated compounds and fragments from fungal walls themselves act as elicitor molecules inducing defense responses, initiating transcription of plant defense genes across the epidermal cell layer (Lee et al 1999; Logemann et al 2001; Assmann and Shimazaki, 1999; Taylor and Assmann, 2001). Lee et al (1999) used the elicitors oligogalacturonic acid (OGA) and chitosan, fragments generated from plant cell walls and fungal degradation, to initiate an oxidative burst in plant cells. The result of this oxidative burst was the activation of the signaling pathways and a change of stomatal aperture overriding or inhibiting the light-regulation of the aperture (Logemann et al, 2001; Lee et al, 1999). The fragments also stimulated up-regulation of defense genes and the synthesis of phenolic compounds evident as increased auto-fluorescence (Assmann and Shimazaki, 1999; Taylor and Assmann, 2001).

Bruchins are also elicitors of plant defense response, triggering increased auto-fluorescence and increased levels of defense compounds (Cooper et al, 2005; Doss, 2005). Bruchin treatment stimulates the accumulation of the phytoalexin, phenolic defense compound, pisatin (Cooper et al, 2005; Doss, 2005). Thordal-Christensen (1997)

showed that HR response of barley leaves to powdery mildew fungus stimulated ROS and phytoalexin production.

Tracking both *Np* phenotypes through their common cellular responses led to the revelation that both originate at the SC. Why would the SC be the locus of two distinct environmental responses? SC are unique to the pods as are both phenotypic responses. The subsidiary cells of the SC are modified epidermal cells distinctively focused around the guard cells (GC). GCs are important environmental sensors not only for guard cell function but also for plant homeostasis. GC light sensitivity, including to UV, mediates stomatal aperture with changes in GC turgor via anion/ion flux (Logemann and Hahlbrock 2001, Assmann and Shimazaki, 1999; Taylor and Assmann, 2001). High temperatures and high light intensity trigger transcription and reorient GC chloroplasts to protect them from UV damage (Logemann and Hahlbrock 2001, Assmann and Shimazaki, 1999; Taylor and Assmann, 2001). GC may be the only surface cells capable of detecting the reduction of UV light and generating a signal to the subsidiary cells and, ultimately, to the epidermal cells. Guard cells contain chloroplasts whose thylakoid membranes allow rapid generation of ROS for defense signals. ROS, especially the membrane permeable and fairly stable hydrogen peroxide, are used as signaling molecules by many organisms (Finkel and Holbrook, 2000; Solomon et al, 1999).

Both *Np* phenotypes required an intact pod and this indicated communication or feedback between the epidermis and the mesophyll was necessary. A similar relationship was demonstrated by Onoe et al (1987) in which rust inoculation of intact oat leaves increased auto-fluorescence, but inoculation of epidermal peels did not. Mesophyll cells were essential for the epidermal cells to produce a defense response even though

pathogen and/or predator encounters took place on the epidermal cell layer and there was no indication the pathogen or predator had contacted the mesophyll. This implied a signal loop where the epidermis communicated with the mesophyll and the mesophyll signaled the epidermis.

In both animals and plants, ROS and  $\text{Ca}^{2+}$  are integrally involved in PCD (Bowler and Fluhr, 2000; Alvarez et al, 1998; Desagher and Martinou, 2000; Hengartner, 2000). Calcium involvement in signaling cascades and cellular growth has been well established. In *Arabidopsis*,  $\text{H}_2\text{O}_2$  activated  $\text{Ca}^{2+}$  channels in guard cells (Pei et al, 2000). Increased concentrations of  $\text{Ca}^{2+}$  signals HR in soybean (Levine et al 1996). Reduction of available  $\text{Ca}^{2+}$  suppressed DNA fragmentation and chromatin condensation in apoptosis-induced oat leaves (Yao et al, 2001).  $\text{Ca}^{2+}$  activates endonucleases involved in DNA cleavage (Yao et al, 2001). ROS are generated by extracellular oxidases in the cell wall and plasma membrane. They can also be generated by intracellular sources such as chloroplast, mitochondria, and peroxisomes (Green and Fluhr, 1995; Mittler et al, 1998; Mehdy, 1994).

As both phenotypes initiated at the SC, where chloroplasts could generate ROS, investigating the presence of  $\text{H}_2\text{O}_2$  in pods indicated spikes of ROS in both phenotypes, and these spikes preceded neoplasm development. Of great interest here was not just that both -UV and bruchin-treated sites tested positive for ROS, but that in 3h post-bruchin treatment the nuclei of the epidermal cells stained strongly for peroxide/peroxidase and by 24h nuclei of the mesophyll were deeply stained. The fact that there was a ROS spike and that ROS was present in the epidermal cell nuclei and later in the mesophyll nuclei could be evidence of a signal transmitted from the epidermis to the mesophyll.

ROS are used as signaling molecules for a number of cellular functions. In seeds, ROS are defensive as well as developmental signaling molecules (Finkel and Holbrook, 2000; Zhang et al, 2001). Low levels of cellular H<sub>2</sub>O<sub>2</sub> in seed activated cell division and elicited transcription of defense genes that signaled distant cells (Levine et al, 1996). ROS initiated PCD in designated cells and a radiated ROS signal induced PCD in adjacent cells. Elimination of the ROS signal reversed PCD in cells (O'Brien et al, 1998; Pennell and Lamb, 1997).

As PCD appeared to be involved in the *Np* phenotypes, I searched for cellular characteristics of PCD using microscopy and molecular techniques. Light microscopy revealed cell shrinkage, cytoplasmic condensation, membrane bound apoptotic bodies, and cell collapse. Apoptotic bodies were evident in cells of *Np* after 48h in -UV, although I never saw this in bruchin treated tissue. The clustering of chloroplasts around the nuclei has not been described before, however, ricinosome formation in senescing tissues has similar characteristics (Schmid et al, 1999). The ricinosomes budded from the ER (Schmid et al, 2001); perhaps this is linked to the ER disruption seen in TEM. TEM revealed mitochondrial swelling, nuclear blebbing, increased cytosolic density and perhaps the loss of ER and the release of ribosomes throughout the cytoplasm matrix. I was not sure what to make of the possible demise of the ER since this has not been linked to early apoptotic events previously. But this disruption of the ER would need to happen at some point in PCD as the cell dismantles itself (Tom Wolpert personal communication). Could this early ER-ribosome disruption be unique to plant apoptosis, or just a feature of the pea *Np* response?

TUNEL assay of bruchin treated and -UV-treated *Np/np* pods, clearly displayed endonuclear nicking in *Np* cells. Nuclear degradation in bruchin treated *Np* tissues amplified over time. Chromatin condensation, not apparent in TEM, is clearly represented in the TUNEL results. In *Np* cells, movement of chromatin to the margin of the nuclear envelope mirrored results reported by Hunot and Flavell, (2001) and discussed as “peripheral-type condensed chromatin”.

Chromatin condensation can take at least two paths. One is the ‘clumping’ of condensed chromatin in a central spot of the nucleus. In the other, the condensed chromatin moves to the edge or perimeter of the nuclear membrane (Hunot and Flavell, 2001). Condensation of the chromatin and its movement to the outer limits of the nuclear envelope as seen in these studies can be reversed. O’Brien et al, (1998) demonstrated that removal of the PCD signal reversed condensation in cells at this level of chromatin condensation and ended the cellular commitment to suicide. This is important because there was evidence of endonuclear DNA nicking in some mesophyll cells in the layer directly beneath the epidermal layer and DAB also stained nuclei of the mesophyll and yet there was no indication of mesophyll cell death. But O’Brien et al, (1998) reported that in cells with as much as 80% condensation of nuclear chromatin, damage could be reversed if the apoptotic signal was withdrawn. In my studies DAB staining indicated that the mesophyll nuclei had elevated ROS levels, and TUNEL indicated DNA nicking in the mesophyll.

Since  $H_2O_2$  was generated in response to bruchin treatment and in tissues exposed to -UV, tests were conducted with compounds that promoted or inhibited ROS production. Of the ROS promoters, only Rose Bengal a singlet oxygen ( $^1O_2$ ) generator,

yielded a bruchin-type reaction, producing site-specific cell division, but only on *Np* pods exposed to -UV conditions.

Singlet oxygen is a highly reactive molecule and can cause cellular damage. Cellular homeostasis is maintained with the metabolism of  $^1\text{O}_2$  to the more stable  $\text{H}_2\text{O}_2$  (Zhang et al 2001). Zhang et al (2001) demonstrated with a colorimetric assay that  $\text{H}_2\text{O}_2$  levels in guard cells increased first in the region of the chloroplasts and the nuclei. RB led to site-specific neoplasm formation mirroring the cellular specificity of bruchin but it did so only on pods exposed to -UV, but not +UV pods. RB was not sufficient for development of SN response. RB reacting on -UV pods did not produce neoplasm over the pod surface reflective of a SN response. RB results indicated that singlet oxygen can directly affect cell division. Chloroplasts can rapidly generate  $^1\text{O}_2$  at the thylakoid membrane (Zhang et al, 2001). The activity of RB was consistent with the theory that neoplasm initiated at the guard cells because guard cells chloroplasts had greater capacity for singlet oxygen generation. The fact that this only takes place on pods exposed to -UV leads to the question: If all that were necessary for development of neoplasm were a ready source of  $^1\text{O}_2$  why didn't the pods grown in +UV conditions develop neoplastic growth following RB application? Could  $^1\text{O}_2$  be fueling a mechanism already up regulated by -UV conditions in the greenhouse or is RB doing something else entirely?

It was hypothesized that an inhibitor of ROS formation would inhibit neoplastic growth. ROS scavenger compounds such as curcumin, catechin, rutin, and ascorbic acid failed to affect the bruchin reaction and these particular compounds also failed to attenuate or enhance SN development. But other compounds tested, while they had no effect on the bruchin reaction, did inhibit SN, including; low doses of DPI, an inhibitor of

NADPH oxidase and peroxidase; jasmonic acid (JA); cAPX, a ROS scavenger; hydrogen peroxide ( $\text{H}_2\text{O}_2$ ), an example of a ROS; Paraquat® and aminotriazole both generators of ROS. Pods, grown in the greenhouse, were treated with these compounds and SN was reduced and in some cases inhibited at the application site. Exogenously modulating ROS levels on pods in -UV conditions led to reduced SN formation but had no effect on the bruchin response. These results provide initial evidence of different ROS sources for each *Np* phenotype. NADPH oxidase appears to be active in the SN response but could not be linked to the bruchin response.

Studies of ozone stress on *Arabidopsis* have elucidated a signaling pathway generating ROS and resulting in cell death (Joo et al, 2005). Ozone stress induced a biphasic oxidative burst in guard cells followed by the epidermal cells. These results appeared very similar to DAB staining of *Np* -UV treated pods. Ozone stress generated increased auto-fluorescence beginning at the GC and radiating to the epidermal cells, as does the *Np* response. Joo et al, (2005) used null mutants to determine that heterotrimeric G protein is essential for activation of intracellular ROS production. Its subunits function both synergistically and separately eliciting ROS signaling. The first part of the response generates rapid endogenous ROS at the chloroplasts in guard cells. This first activation requires both the  $G\alpha$  and  $G\beta\gamma$  complex. Late ROS production, in cells adjacent to the guard cells, is triggered by an extracellular ROS signal generated by membrane associated flavin oxidase NADPH.  $G\alpha$  is necessary and sufficient to produce this late, second ROS peak. The late peak induces cell death. This second ROS spike is inhibited by DPI. Double mutants eradicating NADPH oxidase function abolished ROS and the development of fluorescence in epidermal “pavement” cells but not guard cell chloroplast

(Joo et al, 2005). Could -UV trigger  $G\alpha$  and  $G\beta\gamma$  and intracellular ROS at the chloroplast that then activates  $G\alpha$ , NADPH oxidase, and the generation of extracellular ROS leading to SN on -UV-treated *Np* pods? DPI blocks NADPH oxidase and DPI prevented SN development in -UV treated *Np* pods. RB could feed this pathway by substituting for ROS generated at the thylakoid membrane. RB did not produce neoplasm on +UV pods and DPI did not inhibit bruchin induced neoplasm formation. Bruchin response may not engage NADPH oxidase by acting as an elicitor molecule triggering extracellular ROS or calcium influx. In the cell, ROS or calcium could activate intracellular death cascades as well as a second ROS spike that triggers cell division. Lanthanum competes with calcium, limiting its entry to the cell and consequently eliminating nearly the entire bruchin *Np* phenotype except a slight peroxide staining that is comparable to *np* response.

## Conclusion

The *Np* allele of *Pisum sativum*, common in primitive pea germplasm (Dodds and Matthews 1966) governs a polyphenic response to environmental stimulus, -UV, and the predator biochemical stimulus, bruchin (Nuttall and Lyall 1964; Dodds and Mathews 1966; Bernikov et al. 1992; Doss et al. 1995; Doss et al, 2000). *Np* expression reduces predatory infestation of *Bruchus pisorum* L., pea weevil, (Bernikov, et al. 1992; Doss et al. 2000) and in deep shade or in the green house *Np* conditions neoplastic growth over the entire pod surface (Dodds and Lyall 1964; Dodds and Mathews, 1966). My research has revealed auto-fluorescence as the first discernable response following treatment of *Np* pods with either -UV or bruchin. It has also revealed that an intact pod is necessary for the development of the response. Other defense responses also require an intact host

(Onoe et al. 1987). This suggested communication between the epidermal layer of cells and the mesophyll was essential and necessary. The requirement of an intact pod also indicated the browning at the bruchin treatment site resulted from PCD not necrosis as necrosis would not require a functioning cell (Desagher and Martinou, 2000). This research demonstrated that PCD is a response to bruchin treatment but evidence of SN involving PCD is not as clearly indicated as originally hypothesized. Previous work indicated SN initiated at the SC (Snoad and Mathews, 1969; Burgess and Fleming, 1973). *Pisum* pods have a unique configuration around the guard cells that is not present on the leaf or stem tissues (Snoad and Mathews, 1969; Burgess and Fleming, 1973). The SC are the locus of both *Np* phenotypes. GC are regulatory and environmental sensors for plants (Assmann and Shimazaki, 1999). Small molecules such as  $H_2O_2$  and  $Ca^{2+}$  are integral to cellular responses to pathogens the initiation of defense responses as well as moderating the stomatal aperture for plant homeostasis (Hamilton Bowler and Fluhr, 2000; Levine, 1996; Pei et al, 2000; Thordal-Christensen 1997). Some of these small molecules are readily generated by thylakoid membranes in chloroplasts of guard cells (Zhang et al. 2001).

The pleiotropic character of *Np* may differentially activate different signaling pathways that culminate in cell division. Research indicates both phenotypes utilized unique signaling mechanisms; bruchin response was dependent on an early  $Ca^{2+}$  influx into the cell whereas preliminary results examining SN response pointed toward a signaling pathway that involved NADPH as indicated by the ability of DPI to perturb manifestation of SN. DAB staining revealed the generation of ROS and TUNEL demonstrated DNA nicking an early cellular commitment in PCD.

Preliminary work was done exploring  $\text{Ca}^{2+}$  influx with lanthanum but other methods could expand understanding of  $\text{Ca}^{2+}$  role. The compounds capable of altering the SN response merit further attention. These compounds have provided some initial evidence for each *Np* phenotype activating different sources of ROS such as NADPH oxidase which appears to function in the SN formation in response to -UV but could not be associated with bruchin response.

## Bibliography

- Allan, C.A. and R. Fluhr. 1997. Two distinct sources of elicited reactive oxygen species in tobacco epidermal cells. *The Plant Cell*. 9:1559-1572.
- Alvarez, M.E., R.I. Pennell, P. Meijer, A. Ishikawa, R.A. Dixon, C. Lamb. 1998. Reactive oxygen intermediates mediate a systemic signal network in the establishment of plant immunity. *Cell*. 92:773-784.
- Assmann, S.M., K. Shimazaki. 1999. The multisensory guard cell. Stomatal responses to blue light and abscisic acid. *Plant Physiology*. 119:809-815.
- Balk, J., and C.J. Leaver. 2001. The PET1-CMS mitochondrial mutation in sunflower is associated with premature programmed cell death and cytochrome c release. *The Plant Cell*. 13:1803-1818.
- Berdnikov, V.A., Y.A. Trusov, V.S. Bogdanova, O.E. Kosterin, S.M. Rozov, S.V. Nedel'kina, Y.N. Nikulina. 1992. The neoplastic pod gene (*Np*) maybe a factor for resistance to the pest *Bruchus pisorum* L.. *Pisum Genetic Research Reports*. 24:37-39
- Bowler, C., R. Fluhr. 2000. The role of calcium and activated oxygens as signals for controlling cross-tolerance. *Trends in Plant Science*. 5:6:241-246
- Brenner, C., G. Kroemer. 2000. Mitochondria- the death signal integrators. *Science* 289:5482:1150-1151.
- Burgess, J. and E.N. Fleming. 1973. The structure and development of a genetic tumour of the pea. *Protoplasma*. 76:315-325.
- Cakmak, I.. 2000. Tansley review no. 111: Possible roles of zinn in protecting plant cells from damage by reactive oxygen species. *New Phytol. Review*. 146, 185-205.
- Cooper, L.D., R.P. Doss, R. Price, K. Peterson, J.E. Oliver. 2005. Application of Bruchin B to pea pods results in the up-regulation of CYP93C18, a putative isoflavone synthase gene, and an increase in the level of pisatin, an isoflavone phytoalexin. *Journal of Experimental Botany*. 56:414:1229-1237.
- Desagher, S. and J. Martinou. 2000. Mitochondria as the central control point of apoptosis. *Trends in Cell Biology*. 10:369-377.
- Dodds, Kenneth S. and P. Matthews. 1966. Neoplastic pod in the pea. *J. Hered.* 57:83-85.
- Doss, R.P.. 2005. Treatment of pea pods with Bruchin B results in up-regulation of a gene similar to MtN19. *Plant Physiology and Biochemistry*. 43:225-231.

- Doss, R.P., J.E. Oliver, W.M. Proebsting, S.W. Potter, S.L. Clement, R.T. Williamson, J.R. Carney, E.D. DeVilbiss. 2000. Bruchin: insect- derived plant regulator that stimulates neoplasm formation. PNAS. 97:11: 6218-6223.
- Doss, R., W.M. Proebsting, S.W. Potter, S. L. Clement. 1995. Response of *Np* mutant of pea (*Pisum sativum* L.) to pea weevil (*Bruchus pisorum* L.) oviposition and extracts. Journal of Chemical Ecology. 21:1.
- Fernandes, G. Wilson. 1990. Hypersensitivity: a neglected plant resistance mechanism against insect herbivores. Environ. Entomol. 19:5: 1173-1182.
- Finkel, E. 2001. The mitochondrion: Is it central to apoptosis? Science 292:5517:624-626
- Finkel, T., N. J. Holbrook. 2000. "Oxidants, oxidative stress and the biology of aging" Nature. 408:9:239-247.
- Green, R. and R. Fluhr. 1995. UV-B-induced PR-1 accumulation is mediated by active oxygen species. The Plant Cell 7:203-212.
- Greenberg, J.T.. 1996. Programmed cell death: A way of life for plants. PNAS. 93:12094-12097.
- Groover, A., N. DeWitt, A. Heidel, A. Jones. 1997. Programmed cell death of plant tracheary elements differentiating in vitro. Protoplasma 196:197-211.
- Hamilton, D.W.A., A. Hills, B. Kohler, M.R. Blatt. 2000. Ca<sup>2+</sup> channels at the plasma membrane of stomatal guard cells are activated by hyperpolarization and abscisic acid. PNAS. 97:4967-4972.
- Hengartner, M.O.. 2000. The biochemistry of apoptosis. Nature. 407:770-776.
- Hunot, S., R.A. Flavell. 2001. Death of a monopoly? Science. 292:865-866.
- Jones, A.M.. 2001. "Programmed cell death in development and defense." Plant Physiology 125:94-97.
- Joo, J.H., S. Wang, J.G. Chen, A.M. Jones, N. V. Fedoroff. 2005. Different signaling and cell death roles of heterotrimeric G protein  $\alpha$  and  $\beta$  subunits in the Arabidopsis oxidative stress response to ozone. The Plant Cell. 17:957-970.
- Joza, N., S.A. Susin, E. Daugas, W.L. Stanford, S.K. Cho, C.Y.J. Li, T. Sasaki, A.J. Elia, H.Y.M. Cheng, L. Ravagnan, K.F. Ferri, N. Zamzami, A. Wakeham, R. Hakem, H. Yoshida, Y.Y. Kong, T.W. Mak, J.C. Zuniga-Pflucker, G. Kroemer, J.M. Penninger. 2001. Essential role of the mitochondrial apoptosis-inducing factor in programmed cell death. Nature. 410 29.

Klosterman, S.J., J.J. Choi, L.A. Hadwiger. 2000. Programmed cell death is not mediated by a p53 homolog in *Pisum sativum*. *Physiology and Molecular plant Pathology*. 56:197-206.

Lam, E., N. Kato, and M. Lawton. 2001. "Programmed cell death, mitochondria and the plant hypersensitive response." *Nature* 411.

Lam E., D. Pontier, O. del Pozo. 1999. Die and let live – programmed cell death in plants. *Cell Biology* 21502-21507.

Lee, S., H. Choi, S. Suh, I. Doo, K. Oh, J. Choi, A.T.S. Taylor, P.S. Low, Y. Lee. 1999. Oligogalaturonic acid and chitosan reduce stomatal aperture by inducing the evolution of reactive oxygen species from guard cells of tomato and *Commelia communis*. *Plant Physiology*. 121:147-152.

Levine, A., R.I. Pennell, M.E. Alvarez, R. Palmer, C. Lamb. 1996. Calcium-mediated apoptosis in a plant hypersensitive disease resistance response. *Current Biology*. 6:4:427-437.

Levine, A., R. Tenhaken, R. Dixon, C. Lamb. 1994. H<sub>2</sub>O<sub>2</sub> from the oxidative burst orchestrates the plant hypersensitive disease resistance response. *Cell*. 79:583-593.

Liakopoulos, G., S. Stavrianakou, and G. Karabourniotis. 2001. Analysis of epicuticular phenolics of *Prunus persica* and *Olea europaea* leaves: evidence of the chemical origin of the UV-induced blue fluorescence of stomata. *Annals of Botany*. 87: 641-648.

Logemann E. and K. Hahlbrock. 2001. Crosstalk among stress responses in plants: Pathogen defense overrides UV protection through an inversely regulated ACE/ACE type of light-responsive gene promoter unit. *PNAS*. 99(4):2428-2432.

Mehdy, M. 1994. Active oxygen species in plant defense against pathogens. *Plant Physiology*. 105:467-472.

Mittler, R., and E. Lam. 1995. Identification, characterization, and purification of a tobacco endonuclease activity induced upon hypersensitive response cell death. *The Plant Cell*. 7:1951-1962.

Navarre, D.A., T.J. Wolpert. 1999. Victorin induction of an apoptotic/senescence-like response in oats. *The Plant Cell*. 11:237-249.

Nuttall, V.W. and L.H. Lyall. 1964. Inheritance of neoplastic pod in the pea. *J. Hered.* 55:184-186.

- O' Brien, I.E.W., B.C. Baguley, B.G. Murray, B.A.M. Morris, I.B. Ferguson. 1998. Early stages of the apoptotic pathway in plant cells are reversible. *The Plant Journal*. 13:6:803-814.
- O'Brien, I.E.W., C.P.M. Reutelingsperger, K.M. Holldaway. 1997. Annexin-V and TUNEL use in monitoring the progression of apoptosis in plants. *Cytometry*. 29:28-33.
- Onoe, T., T. Toshikazu, S. Minagawa, H. Sagawa. 1987. Ultrastructural changes of stomata in relation to specificity of rust fungi. *Molecular Determinates of Plant Diseases*. 29-42
- Pei, Z., Y. Murata, G. Benning, S. Thomine, B. Klusener, G.J. Allen, E. Grill, J.I. Schroeder. 2000. Calcium channels activated by hydrogen peroxide mediate abscisic acid signaling in guard cells. *Nature*. 406:731-734.
- Pennell, R.I., and C. Lamb. 1997. Programmed cell death in plants. *The Plant Cell*. 9:1157-1168.
- Potikha, T.S., C.C. Collins, D.I. Johnson, D.P. Delmar, A. Levine. 1999. The involvement of hydrogen peroxide in the differentiation of secondary walls in cotton fibers. *Plant Physiology*. 119:849-858.
- Schmid, M., D.J. Simpson, C. Gietl. 1999. Programmed cell death in castor bean endosperm is associated with accumulation and release of a cysteine endopeptidase from ricinosomes. *PNAS*. 96:14159-14164.
- Schmid, M., D.J. Simpson, H. Sarioglu, F. Lottspeich, C. Gietl. 2001. The ricinosomes of senescing plant tissue bud from the endoplasmic reticulum. *PNAS*. 98:5353-5358.
- Schopfer, P., C. Plachy, G. Frahry. 2001. Release of reactive oxygen intermediates (superoxide radicals, hydrogen peroxide, and hydroxyl radicals) and peroxidase in germinating radish seeds controlled by light, gibberellin, and abscisic acid. *Plant Physiology*. Vol. 125:1591-1602.
- Sedlarova M. and A. Lebeda. 2001. Histochemical detection and role of phenolic compounds in the defense response of *Lactuca ssp* to lettuce downy mildew (*Bremia lactucae*). *J. Phytopathology* 149: 693-697.
- Snoad, Brain and P. Matthews. 1969. Neoplasms of the pea pod. *Chromosomes Today*. 2:126-131.
- Solomon, M., B. Belenghi, M. Pelledonne, A. Levine. 1999. The involvement of cyteine protease inhibitor genes in programmed cell death in plants. 11:431-4444

Taylor, A., S.M. Assmann. 2001. Apparent absence of a redox requirement for blue light activation of pump current in broad bean guard cells. *Plant Physiology*. 125:329-338

Thordal-Christensen, H., Z. Zhang, Y. Wei, D.B. Collinge. 1997. Subcellular localization of H<sub>2</sub>O<sub>2</sub> in plants. H<sub>2</sub>O<sub>2</sub> accumulation in papillae and hypersensitive response during the barley-powdery mildew interaction. *The Plant Journal*. 11:6:1187-1194.

Wang, H., J. Li, R.M. Bostock, D.G. Gilchrist. 1996. Apoptosis: A functional paradigm for programmed cell death induced by host-selective phytotoxin and invoked during development. *The Plant Cell*. 8:375-391.

Yao, N., Y. Tada, P. Park, H. Nakayashiki, Y. Tosa, S. Mayama. 2001. Novel evidence for apoptotic response and differential signals in chromatin condensation and DNA cleavage in Victorian-treated oats. *The Plant Journal*. 28:1:13-26.

Zhang, X., L. Zhang, F. Dong, J. Gao, D.W. Galbraith, C. Song. 2001. Hydrogen peroxide is involved in abscisic acid-induced stomatal closure in *Vicia faba*. *Plant Physiology*. 126:1438-1448.